River Japan, KBT Oriental, or Japan SLC. All animal experiments were performed under the auspices of the Institutional Animal Care and Research Advisory Committee.

BMT

Mice were transplanted as previously described.[20] In brief, after lethal x-ray total body irradiation (TBI) delivered in 2 doses at 4-hour intervals, mice were intravenously injected with 5×10^6 T-cell depleted bone marrow (TCD-BM) cells with or without 2×10^6 splenic T cells on day 0. Isolation of T cells and T-cell depletion were performed using the T-cell isolation kit and anti-CD90 microBeads, respectively, and the AutoMACS (Miltenyi Biotec) according to the manufacturer's instructions. In some experiments, unirradiated B6D2F1 mice were intravenously injected with 12×10^7 splenocytes.[7] Mice were maintained in specific pathogen-free conditions and received normal chow and autoclaved hyperchlorinated water (Ph 4) for the first 3 weeks after BMT and filtered water thereafter. Polymyxin B (Calbiochem) diluted in water was administered by daily oral gavage at a dose of 100 mg/kg from day −4 until day 28 after BMT. Survival after BMT was monitored daily and the degree of clinical GVHD was assessed weekly by a scoring system which sums changes in 5 clinical parameters: weight loss, posture, activity, fur texture, and skin integrity (maximum index = 10) as previously described.[20]

Histologic and immunohistochemical analysis

For pathologic analysis, samples of the small intestine were fixed in 10% neutral-buffered formalin, embedded in paraffin, sectioned, slide mounted, and stained with H&E. Immunohistochemistry was performed as described[21] using rabbit anti-lysozyme (Dako) and rabbit anti-defensin1. Histofine simple stain MAX PO (Rat) kits and subsequently diaminobenzide (DAB) solution (Nichirei Biosciences) was used to generate brown-colored signals. Slides were then counterstained with hematoxylin. Pictures from tissue sections were taken at room temperature using a digital camera (DP72; Olympus) mounted on a microscope (BX51; Olympus). Acute GVHD was assessed by detailed histopathologic analysis using a semiquantitative scoring system.[22]

Preparation and analysis of isolated mouse crypts

Individual crypts were isolated from the small intestine as previously described.[23] Isolated crypts were fixed with 2% paraformaldehyde in PBS for 20 minutes and permeabilized with 0.2% Triton X-100 in PBS for 5 minutes. Crypts were incubated for 1 hour with fluorescein isothiocyanate-conjugated anti-lysozyme (10 μg/mL; Dako), washed 3 times in PBS, followed by incubation for 1 hour with Allexa Fluor 594–conjugated phalloidin (1 U/mL; Invitrogen). Tetramethyl 4,6-diamidino-2-phenylindole (DAPI; 5 μg/mL; Invitrogen) was used to stain the nucleus. Samples were mounted in aqua poly/mount (Polysciences) and examined with a confocal laser-scanning microscope (LSM510; Carl Zeiss).

Enzyme-linked immunosorbent assay

The limulus amebocyte lysate assay QCL-1000 (Lonza) was performed according to the manufacturer's instructions to determine the serum level of lipopolysaccharide (LPS) with a sensitivity of 0.1 EU/mL. All units expressed are relative to the United States reference standard EC-2.

Quantitative real-time PCR analysis

Total RNA was purified using the RNeasy Kit (QIAGEN). cDNA was synthesized using a QuantiTect reverse transcription kit (QIAGEN). Polymerase chain reactions (PCRs) and analyses were performed with ABI PRISM 7900HT SDS 2.1 (Applied Biosystems) using TaqMan universal PCR master mix (Applied Biosystems), and TaqMan gene expression assays (Defa1: Mm02524428_g1, Defa4: Mm00651736_g1, Defa5: Mm00651548_g1, Defa21/Defa22: Mm04206099_gH, Defcr-rs1: Mm00655850_m1, Lyz1: Mm00657323_m1, and Gapdh: Mm99999915_g1; Applied Biosystems). The relative amount of each mRNA was determined using the standard curve method and was normalized to the level of GAPDH in each sample.

Total fecal bacterial DNA extraction

Total DNA was isolated from fecal pellets using a QIAamp DNA stool mini kit (QIAGEN) with bead beating treatment during the cell-lysis step. Briefly, fresh fecal pellets were collected from individual mice; 0.5 g baked 0.1 mm zirconia/silica beads (Biospec Products) and ASL buffer were added to each aliquot. Fecal samples with ASL buffer were incubated at 95°C, and samples were processed for 1 minute at speed 5.5 on Fastprep system (Qbiogene).[24]

PCR amplification of 16S rRNA gene

Bacterial 16S ribosomal RNA (rRNA) genes were amplified with bacterial-universal primers, 27F (5′-AGAGTTTGATCCTGGCTCAG-3′) labeled at the 5′ end with 6-carboxyfluorescein (6-FAM) and 1492R (5′-GGTTACCTTGT TACGACTT-3′).[25] PCR amplification was performed using *EX Taq* (Takara Bio) and the following program: 3 minutes of denaturation at 95°C, 30 cycles of 0.5 minute at 95°C, 0.5 minute at 50°C, 1.5 minute at 72°C, and a final 10 minutes extension step at 72°C in a BiometraT3 thermocycler (Biometra). Amplicons were purified using a QIAquick PCR Purification kit (QIAGEN).

Restriction fragment length polymorphism (RFLP) analysis

The purified DNA products (3 μL) were digested with 10 U of either *Hha*I or *Msp*I (Takara Bio) in a total volume of 10 μL at 37°C for 3 hours. The restriction digest products (2 μL) were mixed with 10 μL deionized formamide and 0.5 μL GeneScan-1200 LIZ standard (Applied Biosystems). The samples were denatured at 95°C for 2 minutes, followed by rapid chilling on ice. The fluorescently labeled fragments (T-RFs) were separated by size on an ABI 3130 genetic analyzer (Applied Biosystems). The electropherograms were analyzed with GeneMapper Version 4.0 software (Applied Biosystems), and the fragment sizes were estimated using the Local Southern method. Each unique RFLP pattern was designated as an operational taxonomic unit (OTU). OTUs with a peak area of less than 0.5% of the total area were excluded from the analysis. Proportion of *E coli* was defined as the ratio of area of OTU for *E coli* to total areas of OTUs. Diversity of the microbial community corresponding to the RFLP banding pattern was calculated using the Simpson index of diversity 1-D ($D = \Sigma pi^2$)[26] and Shannon diversity index H′ ($H' = -\Sigma piln(pi)$)[27] and where pi is the proportion of total number of species made up of its species.

Cloning and sequencing analysis

Internal region of the 16S rRNA genes were amplified using 27F and 806R (5′-GGACTACCAGGGTATCTAAT-3′) primers, and were transformed using TOPO TA Cloning Kit with TOP10 *E coli* (Invitrogen). The nucleotide sequences of inserts were determined using the M13 forward and reverse primers. All sequences were examined for possible chimeric artifacts by the Chimera check with Bellerophon Version 3. After eliminating chimeric sequences, the partial 16S rRNA sequences were compared with the sequences in the Ribosomal Database Project and GenBank, using the BLAST program (http://www.ncbi.nlm.nih.gov/BLAST/). Cloned sequences were identified as representing the species or phylotype of the sequence with the highest matching score. Sequences with less than 98% identity with a GenBank sequence were defined as a new phylotype. In addition, we checked whether the sequenced clones had the correct T-RFs compared with the sequence information.

Microbiologic analysis of bacterial translocation

The livers and mesenteric lymph nodes (mLNs) isolated from mice that had received transplants were removed aseptically and homogenized in 1 mL saline. Then, 500 μL of homogenate was transferred into a tube containing 4.5 mL of saline and used to perform 4 serial dilutions. From this dilution, 100 μL aliquots were cultured aerobically on blood agar and LB agar plates (Difco) for 24 hours at 37°C in room air supplemented with 10% CO_2. Colony-forming units (CFUs) were counted and adjusted per organ. Bacteria were identified by biochemical profiles.

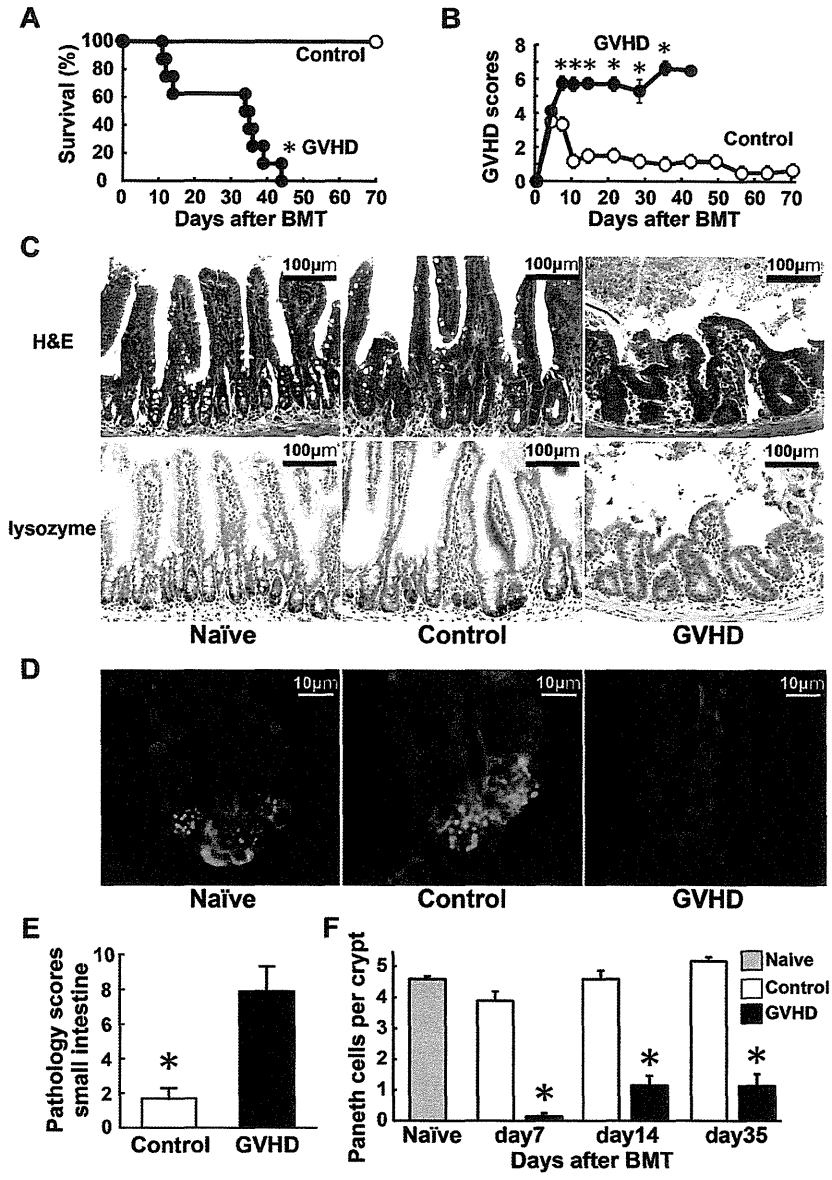

Figure 1. Paneth cell injury in GVHD. Lethally irradiated B6D2F1 mice were transplanted with 5×10^6 TCD BM cells without (control group, n = 6) or with 2×10^6 T cells (GVHD group, n = 12) from MHC-mismatched B6 donors on day 0. (A-B) Survival (A) and clinical GVHD scores (B) means ± SE are shown. Data from 2 independent experiments were combined. (C-F) Small intestines were isolated from mice 7 days after BMT. (C) Top panels: histology of the small intestine stained with H&E. Bottom panels: Lysozyme staining (brown). Magnification:100×. Bars, 100 μm. (D) Confocal cross-sectioning of the isolated small intestinal crypt. Lysozyme (green) is expressed by Paneth cells. Tetramethyl DAPI (blue) stains the nucleus and phalloidin (red) stains F-actin. Magnification: 1000×. Bars, 10 μm. (E) Pathology scores of the small intestine (mean ± SE, n = 3-6 / group). (F) Quantification of Paneth cells per crypt (mean ± SE, n = 3-6 / group; $^*P < .05$).

Statistical analysis

Mann-Whitney *U* tests were used to compare data, the Kaplan-Meier product limit method was used to obtain survival probability, and the log-rank test was applied to compare survival curves. To determine the statistically significant correlation, the Spearman rank correlation coefficient (R) was adopted. All tests were performed with SigmaPlot Version 10.0 software. $P < .05$ was considered statistically significant.

Accession numbers

Sequence data are available in the GenBank (http://www.ncbi.nih.gov/genbank) under the accession number 1509996.

Results

Paneth cell damage and decreased expression of α-defensins in GVHD

We evaluated whether Paneth cells could be damaged during GVHD. Lethally irradiated B6D2F1 (H-$2^{b/d}$) mice received 5×10^6 TCD-BM cells (control group) or these cells plus 2×10^6 T cells (GVHD group) from major histocompatibility complex (MHC)–mismatched B6 (H-2^b) donors on day 0. The allogeneic animals developed severe GVHD and all of these mice died within 50 days after BMT, whereas all TCD-BM controls survived through this period (Figure 1A). The surviving allogeneic animals showed significantly more severe signs of GVHD than controls, as assessed by clinical GVHD scores[20] (Figure 1B). Pathologic analysis of the small intestine 7 days after BMT showed mostly normal architecture in controls, whereas severe blunting of villi and inflammatory infiltration were observed in the GVHD group (Figure 1C). Paneth cells, which are typically identified microscopically by their location in the crypts and by the large granules occupying most of their cytoplasm, were hardly observed in the GVHD group. Immunohistochemical analysis for lysozyme, which indicates the presence of Paneth cells, confirmed loss of Paneth cells in the GVHD group, but not in controls (Figure 1C). Confocal cross-sectioning of individual crypts isolated from the small intestine further confirmed Paneth cell loss in these mice (Figure 1D). In mice with GVHD, GVHD pathology scores were significantly higher (Figure 1E), whereas numbers of Paneth cells

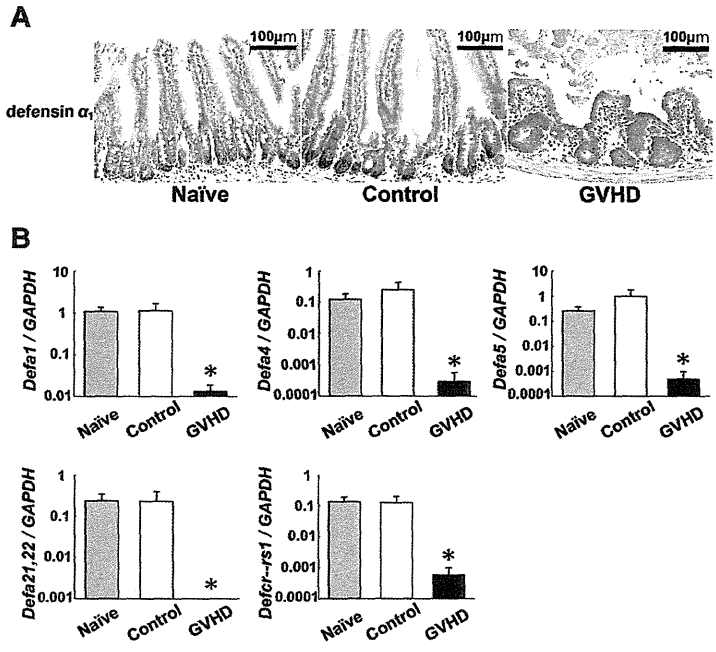

Figure 2. Decreased expression of Paneth cell–derived α-defensins in GVHD. Lethally irradiated B6D2F1 mice were transplanted with 5×10^6 TCD BM without (control group) or with (GVHD group) 2×10^6 T cells from B6 donors. Small intestines were isolated from mice 7 days after BMT. (A) Immunohistochemical staining for defensin α_1 (brown). Magnification: 100×. Bars, 100 μm. (B) RNA was extracted from samples and quantitative real-time PCR analysis for enteric defensins including *Defa1*, *Defa4*, *Defa5*, *Defa21,22*, and *Defcr-rs1* was performed (n = 6 / group). Data are representative of 2 similar experiments and are shown as mean ± SE (*$P < .05$).

were significantly and constantly lower compared with those in controls after BMT (Figure 1F).

α-Defensins are the major antimicrobial peptides produced by Paneth cells.[23] We evaluated the expression levels of enteric defensin families in the small intestines. Defensin α_1 expression was limited in Paneth cells in the crypts of naive mice (Figure 2A). Expression of defensin α_1 was preserved in controls 7 days after BMT but was severely suppressed in mice with GVHD. Quantitative real-time PCR analysis of the terminal ileum confirmed the reduced expression of *defensin-*α_1 *(Defa1)* and other enteric defensin family members, including *Defa5*, *Defa21,22*, and *defensin α-related sequence 1 (Defa-rs1)* in the small intestine of GVHD mice (Figure 2B). These results demonstrate that GVHD targets Paneth cells and limits the expression of Paneth cell–derived defensin family members.

Perturbation of normal intestinal microbiota in GVHD

Paneth cell–derived α-defensins are essential regulators of the microbiota composition in the intestine.[11] α-defensins have selective bactericidal activity against noncommensals, whereas exhibiting minimal bactericidal activity against commensals.[28,29] We therefore hypothesized that the reduced expression of α-defensins results in dysbiosis in the intestinal microbial community. To test this hypothesis, we evaluated changes in the gut flora during the course of GVHD in a B6 → B6D2F1 murine model of BMT without administering any antibiotic or immunosuppressive drugs. Before and after BMT, fecal pellets were collected from each mouse once per week. The composition of the intestinal microflora was determined by RFLP analysis of bacteria-specific 16S rRNA genes that were constructed from each sample of fecal pellets.[30,31] Representative RFLP analysis is shown in Figure 3A. Each unique RFLP pattern is designated by an OTU that corresponds to specific species of bacteria. The peak height of each OTU indicates its relative quantity among the intestinal microflora and the number of OTUs indicates the diversity of flora. Before BMT, multiple OTUs were observed with little interindividual variation among the RFLP patterns (Figure 3A left panels). Seven days after BMT, numbers of OTUs were slightly decreased with little changes in the RFLP patterns in controls (Figure 3A right top panels); however, in the mice with GVHD, the number of OTUs decreased and the peak heights of OTUs were markedly reduced, with the exception of an aberrantly high peak at 368 bp (Figure 3A right bottom panels). Sequence analysis of subclones from a representative animal from GVHD group showed that proportions of both Firmicutes and Bacteroidetes, which are the major enteric commensals,[12,15] were decreased in mice with GVHD on day 7 compared with those before BMT (Firmicutes; 22.9% vs 52.1%, Bacteroidetes; 2.1% vs 13.5%, respectively).

These compositional changes in the intestinal microflora were consistently observed in all mice with GVHD. Diversity of the microbial community, which corresponds to the RFLP banding patterns, was significantly reduced in mice with GVHD at all time points, as assessed by the Simpson index of diversity,[26] Shannon diversity index,[27] and the number of OTUs counted (Figure 3B-D).

Overwhelming outgrowth of *E coli* in mice with GVHD

A single high peak at 368bp was noted in mice with GVHD (Figure 3A arrows). To identify the bacteria included at this OTU, plasmid DNA from the corresponding clone was purified. DNA sequencing showed a high similarity to 16S rRNA from *E coli* with a similarity rate of more than 99.5%. The proportion of *E coli* in the microbiota, which was defined as the ratio of the area of OTU for *E coli* to the total areas of all OTUs, was dramatically higher 7 days after BMT and remained higher in mice with GVHD throughout the entire observation period; however, *E coli* remained to be a small portion of the microbial population in controls (Figure 3E). Next, we evaluated whether the high levels of *E coli* in the intestine could be associated with the development of systemic infection in mice with GVHD. Seven days after BMT, mLNs and livers were harvested. *E coli* was identified from samples taken from mice with GVHD, but not the controls. The number of CFUs of *E coli* was significantly higher in the mLNs and liver of mice with GVHD than those in controls (Figure 3F-G). Serum LPS levels were also significantly higher in mice with GVHD than in controls (Figure 3H).

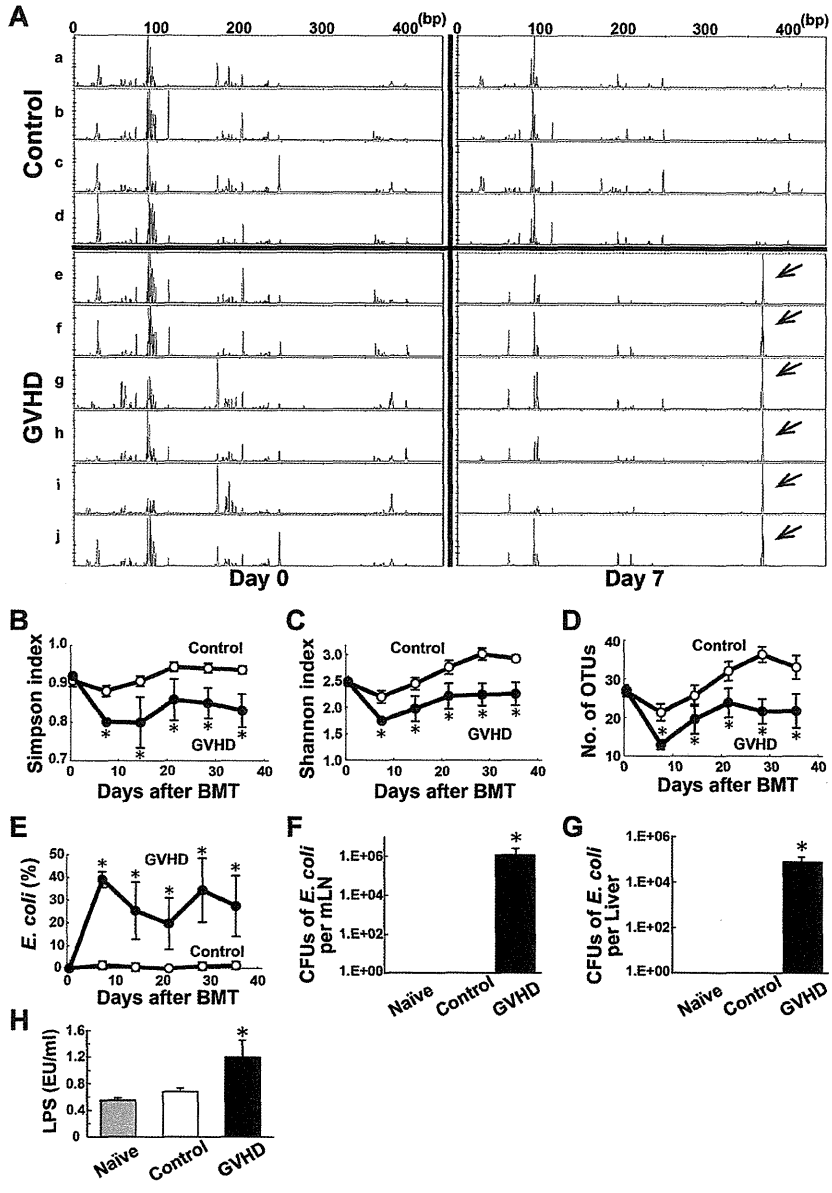

Figure 3. Perturbation of normal intestinal microbiota in GVHD. Fecal pellets were collected before and after a B6 → B6D2F1 BMT weekly and intestinal microbiota was characterized by RFLP analysis of 16S rRNA gene libraries constructed from each sample of fecal pellets and digested with *Hhal* (n = 6 / group). (A) Representative RFLP patterns are shown in control group (a-d) and GVHD group (e-j). Left panels indicate before BMT; right panels, 7 days after BMT. Arrows indicate an OTU for *Escherichia coli*. (B-D) Time course changes in flora diversity after BMT determined by using Simpson index (B), Shannon index (C), and numbers of OTUs (D). (E) Time course changes in the proportion of *E coli*. (F-G) Samples of mLNs and liver were harvested on day 7 and CFUs of *E coli* were enumerated by the culture-based and microbiologic identification method. (H) Serum LPS levels on day 7. Data are representative of 3 similar experiments and are shown as mean ± SE (*$P < .05$).

The composition of intestinal microflora in animals can differ depending on the environment and other factors.[32] Therefore, we used mice purchased from multiple vendors; however, the resulting patterns of dysbiosis were similar, regardless of the origin source of the mice. In addition, we found similar changes in the intestinal microbiota of another haplotype, the mismatched B6 → B6C3F1 (H-$2^{b/k}$) model of BMT. Diversity of intestinal flora was lost with an outgrowth of *E coli* 7 days after BMT and thereafter only in mice with GVHD (data not shown).

Association between changes in intestinal microbiota and GVHD severity

Further studies were conducted to determine whether there could be an association between the magnitude of changes observed in the intestinal flora and GVHD severity. Diversity of the flora, as determined by the Simpson index, Shannon index, and the number of OTUs was inversely correlated with GVHD severity (Figure 4A-C). On the other hand, the proportion of *E coli* in the intestinal flora was positively correlated with GVHD severity (Figure 4D).

Delayed alteration in intestinal microbial diversity after MHC-matched BMT

To further confirm that our observations were not strain or model dependent, we evaluated whether the observed changes in the intestinal flora could be observed in a clinically relevant, MHC-matched, and minor histocompatibility antigen-mismatched C3H.Sw (H-2^b) → B6 (H-2^b) model of BMT, in which GVHD developed more slowly and was less severe compared with the MHC-mismatched models of GVHD (Figure 5A-B).[33] Again, normal microbial diversity was lost in mice with GVHD and *E coli* levels were higher at 2 weeks after BMT and thereafter (Figure 5C-F). Thus, changes in the intestinal microbiota occurred more slowly in this model, at least compared with the MHC-mismatched model of GVHD; furthermore, the changes occurred in parallel with the

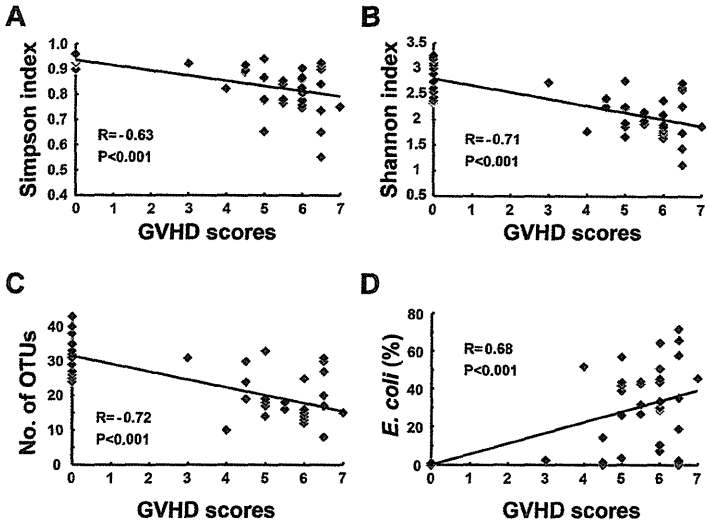

Figure 4. Correlation between the degree of flora changes and GVHD severity. Lethally irradiated B6D2F1 mice were transplanted with TCD BM with T cells from B6 donors (n = 6 / group). Fecal pellets were collected at day 0 and weekly thereafter and intestinal microbiota was characterized by RFLP analysis. Clinical GVHD scores and various parameters of the flora diversity and the proportion of *E coli* in the intestinal flora at various time points from each mice were plotted. Correlations of GVHD clinical scores and Simpson index (A), Shannon index (B), numbers of OTUs (C), and proportion of *E coli* (D). The regression line was plotted with all data. Data from 2 independent experiments were combined. R: correlation coefficient.

slower development of GVHD. It should be noted that normal flora diversity was recovered and *E coli* returned to a normally small population among the intestinal microbiota late after BMT, as GVHD severity reduced. No mortality was observed in allogeneic animals after regaining normal intestinal flora.

Loss of Paneth cells and the dysbiosis by a mechanism independent on conditioning

We addressed whether GVHD mediates Paneth cell injury and the alteration of the composition of the intestinal flora by a mechanism dependent on radiation-induced intestinal tract damage in the B6 → B6D2F1 BMT model without conditioning, as previously described.[7] Unirradiated B6D2F1 mice were intravenously injected with 12×10^7 splenocytes from syngeneic or allogeneic B6 donors on day 0. In this model, GVHD occurred early after BMT at a peak around day 20 but was spontaneously improved (Figure 6A-C). Numbers of Paneth cells were markedly reduced 2 weeks after BMT but gradually returned to normal levels thereafter in allogeneic animals (Figure 6D). The changes in the intestinal microbiota occurred in parallel with the degree of GVHD severity and Paneth cell injury; normal microbial diversity was lost with the outgrowth of *E coli*, but was gradually restored later after BMT in allogeneic animals (Figure 6E-H).

Oral administration of antibiotics inhibited the outgrowth of *E coli* and ameliorated GVHD

Finally, we evaluated whether modifying the enteric flora using oral antibiotics could ameliorate GVHD. Lethally irradiated B6D2F1 mice were transplanted with 5×10^6 TCD BM cells with or without 2×10^6 T cells from B6-Ly5.1 (CD45.1$^+$) donors. Polymyxin B (PMB), an antibiotic primarily effective against gram-negative bacteria, was administered by daily oral gavage at a dose of 100 mg/kg from day −4 until day 28 after BMT. Analysis of fecal pellets 7 days after BMT showed that the outgrowth of *E coli* was inhibited in mice treated with PMB compared with those treated with diluent (Figure 7A). PMB suppressed the outgrowth of *E coli* during PMB treatment; however, *E coli* levels increased after cessation of PMB treatment (Figure 7B). Notably, administration of PMB significantly reduced mortality and morbidity of GVHD (Figure 7C-D). Donor (CD45.1$^+$) T-cell expansion (Figure 7E) and pathology scores of the small intestine (Figure 7F) were significantly reduced in PMB-treated mice compared with those in controls.

Discussion

Intestinal GVHD is critical for determining the outcome of allogeneic BMT. Paneth cells are essential regulators of the

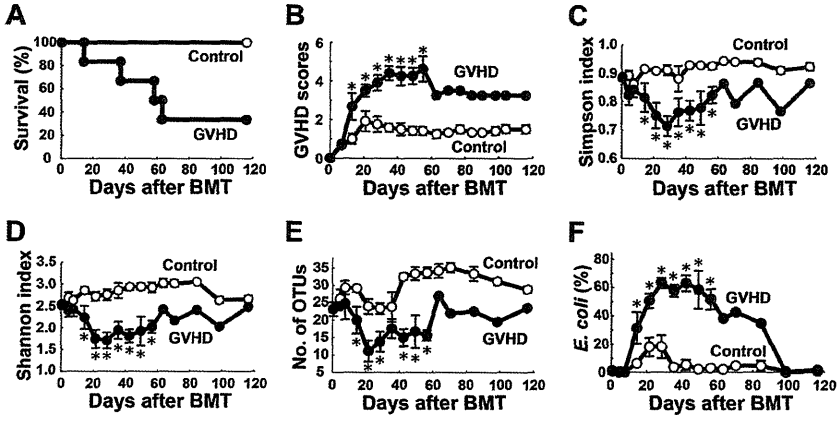

Figure 5. Delayed impairment of the intestinal ecology after MHC-matched BMT. B6 mice were transplanted with 5×10^6 TCD BM without (control group) or with (GVHD group) 2×10^6 T cells from C3H.Sw donors after 12 Gy TBI (n = 6/group). (A-B) Survival (A) and clinical GVHD scores (B, mean ± SE) in control group and GVHD group. Data are representative of 3 similar experiments. (C-F) Fecal pellets were collected once per week after BMT and intestinal microflora was characterized by RFLP analysis of 16S rRNA genes constructed from each sample of fecal pellets and digested with *Hha*I. Time course changes in flora diversity determined by Simpson index (C), Shannon index (D), and numbers of OTUs (E). (F) Time course changes in the proportion of *E coli*. Data are representative of 3 similar experiments and are shown as mean ± SE (*$P < .05$).

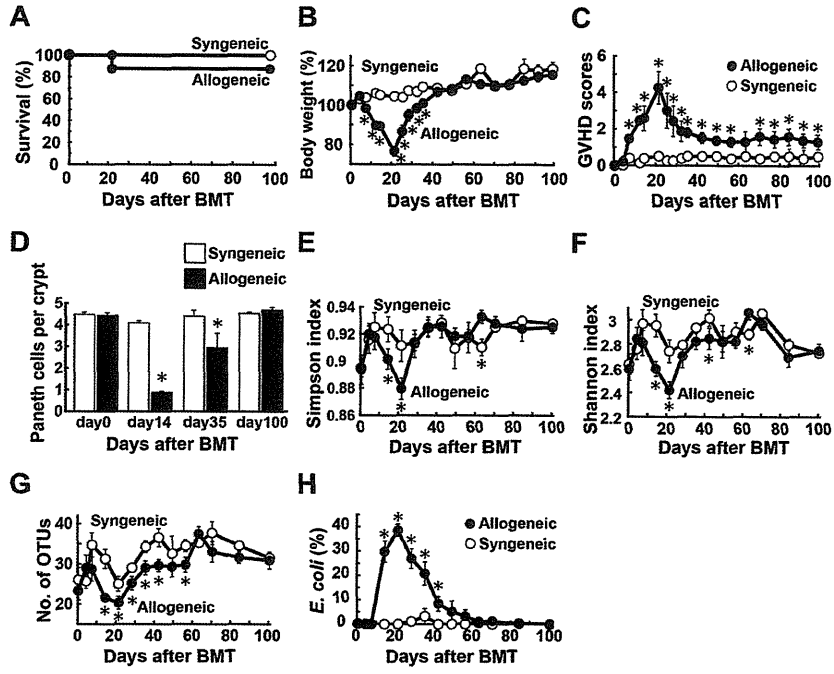

Figure 6. Paneth cell injury and the dysbiosis developed by a mechanism independent on conditioning. Unirradiated B6D2F1 mice were transplanted with 12×10^7 splenocytes from syngeneic or allogeneic MHC-mismatched B6 donors on day 0 (n = 6/group). Survival (A), changes in body weight (B, mean ± SE), clinical GVHD scores (C, mean ± SE), and (D) quantification of Paneth cells per crypt in the small intestine were shown. (E-H) Fecal pellets were collected before and after BMT weekly and intestinal microbiota was characterized by RFLP analysis of 16S rRNA gene libraries constructed from each sample of fecal pellets and digested with *Hhal*. Time course changes in flora diversity determined by using Simpson index (E), Shannon index (F), numbers of OTUs (G), and the proportion of *E coli* (H). Data from 2 independent experiments were combined and are shown as mean ± SE.

composition of commensal microbiota in the intestine, and they maintain the intestinal microbial environment by secreting various microbial peptides. In this study, we found that damage to Paneth cells by GVHD results in dramatically reduced expression of α-defensins in the small intestines and perturbed normal intestinal environment. These changes occurred in the absence of conditioning irradiation, thus indicating a mechanism dependent on allogeneic T-cell responses. However, Paneth cell loss occurred earlier and more prolonged in mice receiving irradiation than in unirradiated mice, suggesting that conditioning enhanced Paneth cell damage directly and indirectly by accelerating GVHD. The diversity of the intestinal microflora was lost with overwhelming expansion of specific bacteria, such as *E coli*, which are normally a very small proportion of the intestinal microbial communities. Paneth cells secret α-defensins into the intestinal lumen within minutes after sensing gram-negative and gram-positive bacteria and their components, such as LPS, through activation of pattern recognition receptors.[23,34] α-defensins are the most potent antimicrobial peptides and account for 70% of the bactericidal peptide activity released from Paneth cells.[11,23] α-Defensins are released in the small bowel lumen and persist as intact and functional forms throughout the intestinal tract.[35] Thus, they shape the composition of the microbiota in the entire intestine. Importantly, α-defensins have selective bactericidal activity against noncommensals, such as *Salmonella enterica*, *E coli*, *Klebsiella pneumoniae*, and *Staphylococcus aureus*, although exhibiting minimal bactericidal activity against commensals.[28,29] Such bacteria-dependent bactericidal activities of α-defensins are in tune with intestinal environment and may explain why the absence of α-defensins causes the alterations in the intestinal microbiota in GVHD. Because commensals have a profound influence on nutritional, physiologic, and metabolic function of the host,[14,36,37] reduction of commensals may have ill effects on the host with GVHD. In this study, *E coli* was the dominant enteric microbe in mice with GVHD among multiple strains of mice. However, the dominant species may differ between studies because of the differences in several factors, including differences in the maintenance protocols used to feed and care for the experimental animals.[32] Nonetheless, our study confirms and further extends a recent study showing the intestinal flora change, with an increase in gram-negative *Enterobacteriaceae* family members including *E coli*, after allogeneic BMT in mice.[18]

Alteration of the intestinal microbiota has been shown in experimental and clinical inflammatory bowel diseases, allergies, diabetes, and obesity.[13,38-42] This study provides several lines of evidence that suggest a close association between dysbiosis and GVHD. Mice without GVHD maintained normal microbiota after BMT, and dysbiosis only occurred in mice with GVHD, independent of the murine models used. The normal intestinal environment was never restored as long as severe GVHD persisted, but was restored when tolerance was induced after transplant. In mice with GVHD, the degree of changes to the microflora was significantly correlated to GVHD severity and MHC disparity between the donor and recipient. Furthermore, modifying enteric flora by oral administration of antibiotics inhibited the outgrowth if *E coli* and ameliorated GVHD. The flora shift toward the widespread prevalence of gram-negative bacteria increases the translocation of LPS, the major component of the outer membrane of gram-negative bacteria, into systemic circulation and further accelerates GVHD by stimulates production of inflammatory cytokines, such as TNF-α and IL-1, which are critical effector molecules that mediate GVHD.[22,43-45] Thus, GVHD and the dysbiosis can lead to a positive feedback loop that increases the translocation of LPS, thereby resulting in further cytokine production, progressive intestinal injury, and systemic GVHD acceleration. Earlier seminal studies in the 1960s-1970s suggested that GVHD is reduced in germfree mice or by treatment with poorly absorbable antibiotics.[3-6] A recent study also demonstrated that modifying the enteric flora using a probiotic microorganism reduced GVHD in mice.[46] Thus, our study again highlights an important role of oral antibiotics administration on GVHD. Our study demonstrated that dominant bacteria in the intestinal microbiota cause systemic infection. There was a microbiologic evidence of infection in mice with severe GVHD and a correlation between severity of infection and GVHD, thus suggesting that severe bacteremia, probably caused by the translocation of enteric bacteria, can also contribute to GVHD mortality, as previously suggested.[6,46] Indeed, septicemia by gram-negative rods

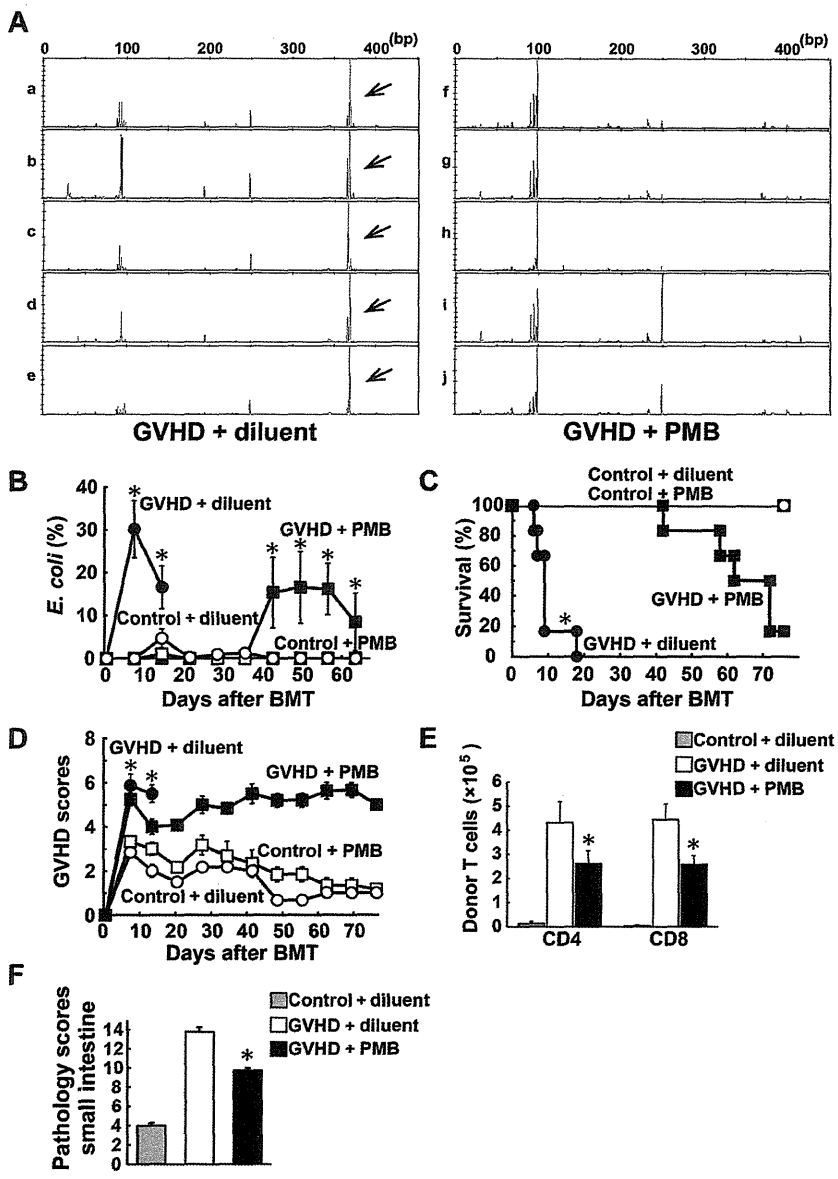

Figure 7. Oral administration of polymyxin B ameliorated GVHD. Lethally irradiated B6D2F1 mice were transplanted with 5×10^6 TCD BM without or with 2×10^6 T cells from B6 or B6-Ly5.1 (CD45.1$^+$) donors. Polymyxin B (PMB; 100 mg/kg) or diluent was administered by daily oral gavage from day −4 until day 28 after BMT. (A) Fecal pellets were collected once per week after BMT and intestinal microflora was characterized by RFLP analysis of 16S rRNA genes constructed from each sample of fecal pellets and digested with *Hha*I. Representative RFLP patterns are shown in mice with GVHD receiving diluent (a-e) and those with PMB (f-j) 7 days after BMT. Arrows indicate an OTU for *E coli*. (B) Time course changes in the proportion of *E coli* (n = 6-12 / group). Survival (C) and clinical GVHD scores (D, mean ± SE) after BMT are shown (n = 6-12/group). Data from 2 independent experiments were combined. (E) Numbers of donor (CD45.1$^+$) T cells in mLNs on day 5 (n = 20/group). (F) Pathology scores of the small intestine on day 7 (n = 20/group). Data from 3 independent experiments were combined and are shown as mean ± SE (*$P < .05$).

is one of the most frequent causes of death in patients with severe intestinal GVHD.

There are other interfaces that exist between the environment and the host, such as the skin and airways. Epithelial cells in these tissues can also release antimicrobial peptides such as β-defensins in response to bacteria and LPS.[47] GVHD-mediated epithelial cell damage of these tissues may also impair the local secretion of antimicrobial peptides, leading to aberrant overgrowth of pathogens and development of dermal infections or pneumonia, which are frequently observed in patients with GVHD. Furthermore, the development of these pathologic conditions may be associated with the unique tissue specificity of GVHD for tissues that are in contact with high microbial loads, such as the skin, liver, intestine, and lung.

Intestinal epithelial cells are continuously regenerated from ISCs, which are required to regenerate damaged sections of the intestinal epithelium.[48] Paneth cells are derived from ISCs and serve as a niche for ISCs.[8] Our previous[7] and current studies addressed intestinal GVHD at the cellular level, and demonstrated that ISCs and their niche Paneth cells could survive pretransplant conditioning and regenerate injured epithelium by conditioning in the absence of GVHD. However, both ISCs and Paneth cells are targeted by GVHD, resulting in an impairment of the physiologic repair mechanisms of injured epithelium, although it remains to be elucidated whether Paneth cell loss is induced by direct cytotoxicity to Paneth cell itself or secondary to the loss of ISCs. This phenomenon may explain the prolonged and refractory nature of clinical intestinal GVHD. These new insights will help to establish new therapeutic strategies that can be used to prevent and treat GVHD and related infections and improve the clinical outcome of allogeneic BMT.

Acknowledgments

This study was supported by grants from Japan Society for the Promotion of Science (JSJP) KAKENHI (23659490 to T.T., 23390193 to T.A., and 22592029 to K.N.), Health and Labor Science Research Grants (T.T.), the Foundation for Promotion of Cancer Research (Tokyo, Japan; to T.T.), the Knowledge Cluster, Sapporo Bio-S from Ministry of

Education, Culture, Sports, Science and Technology (MEXT; Tokyo, Japan; to T.A.), Yakult Bio-Science Foundation (Tokyo, Japan; to Y.E.), and SENSHIN Medical Research Foundation (to T.T.).

Authorship

Contribution: Y.E. and T.T. developed the conceptual framework of the study, designed the experiments, conducted studies, analyzed data, and wrote the paper; S.T., H.O., S. Shimoji, K.N., H.U., S. Shimoda, and H.I. conducted experiments; and N.S., T.A., and K.A. supervised experiments.

Conflict-of-interest disclosure: The authors declare no competing financial interests.

Correspondence: Takanori Teshima, Center for Cellular and Molecular Medicine, Kyushu University Hospital, 3-1-1 Maidashi, Higashi-ku, Fukuoka 812-8582, Japan; e-mail: tteshima@cancer.med.kyushu-u.ac.jp.

References

1. Bossaer JB, Hall PD, Garrett-Mayer E. Incidence of vancomycin-resistant enterococci (VRE) infection in high-risk febrile neutropenic patients colonized with VRE. *Support Care Cancer.* 2010; 19(2):231-237.
2. Winston DJ, Gale RP, Meyer DV, Young LS. Infectious complications of human bone marrow transplantation. *Medicine.* 1979;58(1):1-31.
3. van Bekkum D, Vos O. Treatment of secondary disease in radiation chimaeras. *Int J Radiat Biol.* 1961;3:173-181.
4. Jones JM, Wilson R, Bealmear PM. Mortality and gross pathology of secondary disease in germ-free mouse radiation chimeras. *Radiation Res.* 1971;45(3):577-588.
5. van Bekkum DW, Roodenburg J, Heidt PJ, van der Waaij D. Mitigation of secondary disease of allogeneic mouse radiation chimeras by modification of the intestinal microflora. *J Nat Cancer Inst.* 1974;52(2):401-404.
6. Heit H, Heit W, Kohne E, Fliedner TM, Hughes P. Allogeneic bone marrow transplantation in conventional mice: I. Effect of antibiotic therapy on long term survival of allogeneic chimeras. *Blut.* 1977;35(2):143-153.
7. Takashima S, Kadowaki M, Aoyama K, et al. The Wnt agonist R-spondin1 regulates systemic graft-versus-host disease by protecting intestinal stem cells. *J Exp Med.* 2011;208(2):285-294.
8. Sato T, van Es JH, Snippert HJ, et al. Paneth cells constitute the niche for Lgr5 stem cells in intestinal crypts. *Nature.* 2011;469(7330):415-418.
9. Selsted ME, Harwig SS. Determination of the disulfide array in the human defensin HNP-2. A covalently cyclized peptide. *J Biol Chem.* 1989; 264(7):4003-4007.
10. Ganz T, Selsted ME, Lehrer RI. Defensins. *Eur J Haematol.* 1990;44(1):1-8.
11. Salzman NH, Hung K, Haribhai D, et al. Enteric defensins are essential regulators of intestinal microbial ecology. *Nat Immunol.* 2010;11(1):76-83.
12. Eckburg PB, Bik EM, Bernstein CN, et al. Diversity of the human intestinal microbial flora. *Science.* 2005;308(5728):1635-1638.
13. Qin J, Li R, Raes J, et al. A human gut microbial gene catalogue established by metagenomic sequencing. *Nature.* 2010;464(7285):59-65.
14. Hill DA, Artis D. Intestinal bacteria and the regulation of immune cell homeostasis. *Ann Rev Immunol.* 2010;28:623-667.
15. Zoetendal EG, Akkermans AD, De Vos WM. Temperature gradient gel electrophoresis analysis of 16S rRNA from human fecal samples reveals stable and host-specific communities of active bacteria. *Appl Environ Microbiol.* 1998;64(10): 3854-3859.
16. Kurokawa K, Itoh T, Kuwahara T, et al. Comparative metagenomics revealed commonly enriched gene sets in human gut microbiomes. *DNA Res.* 2007;14(4):169-181.
17. Hooper LV, Macpherson AJ. Immune adaptations that maintain homeostasis with the intestinal microbiota. *Nature Rev Immunol.* 2010;10(3):159-169.
18. Heimesaat MM, Nogai A, Bereswill S, et al. MyD88/TLR9 mediated immunopathology and gut microbiota dynamics in a novel murine model of intestinal graft-versus-host disease. *Gut.* 2010; 59(8):1079-1087.
19. Ubeda C, Taur Y, Jenq RR, et al. Vancomycin-resistant Enterococcus domination of intestinal microbiota is enabled by antibiotic treatment in mice and precedes bloodstream invasion in humans. *J Clin Invest.* 2010;120(12):4332-4341.
20. Cooke KR, Kobzik L, Martin TR, et al. An experimental model of idiopathic pneumonia syndrome after bone marrow transplantation. I. The roles of minor H antigens and endotoxin. *Blood.* 1996;88: 3230-3239.
21. Asakura S, Hashimoto D, Takashima S, et al. Alloantigen expression on non-hematopoietic cells reduces graft-versus-leukemia effects in mice. *J Clin Invest.* 2010;120(7):2370-2378.
22. Teshima T, Ordemann R, Reddy P, et al. Acute graft-versus-host disease does not require alloantigen expression on host epithelium. *Nat Med.* 2002;8(6):575-581.
23. Ayabe T, Satchell DP, Wilson CL, Parks WC, Selsted ME, Ouellette AJ. Secretion of microbicidal alpha-defensins by intestinal Paneth cells in response to bacteria. *Nat Immunol.* 2000;1(2): 113-118.
24. Li F, Hullar MA, Lampe JW. Optimization of terminal restriction fragment polymorphism (TRFLP) analysis of human gut microbiota. *J Microbiol Methods.* 2007;68(2):303-311.
25. Hayashi H, Takahashi R, Nishi T, Sakamoto M, Benno Y. Molecular analysis of jejunal, ileal, caecal and recto-sigmoidal human colonic microbiota using 16S rRNA gene libraries and terminal restriction fragment length polymorphism. *J Med Microbiol.* 2005;54(Pt 11):1093-1101.
26. Simpson EH. Measurement of diversity. *Nature.* 1949;163:688.
27. Shannon C. A mathematical theory of communication. *Bell System Technol J.* 1948;27:379-423.
28. Ouellette AJ, Hsieh MM, Nosek MT, et al. Mouse Paneth cell defensins: primary structures and antibacterial activities of numerous cryptdin isoforms. *Infect Immun.* 1994;62(11):5040-5047.
29. Masuda K, Sakai N, Nakamura K, Yoshioka S, Ayabe T. Bactericidal activity of mouse alpha-defensin cryptdin-4 predominantly affects noncommensal bacteria. *J Innate Immun.* 2011;3(3): 315-326.
30. Liu WT, Marsh TL, Cheng H, Forney LJ. Characterization of microbial diversity by determining terminal restriction fragment length polymorphisms of genes encoding 16S rRNA. *Appl Environ Microbiol.* 1997;63(11):4516-4522.
31. Hayashi H, Sakamoto M, Benno Y. Phylogenetic analysis of the human gut microbiota using 16S rDNA clone libraries and strictly anaerobic culture-based methods. *Microbiol Immunol.* 2002; 46(8):535-548.
32. Ivanov II, Atarashi K, Manel N, et al. Induction of intestinal Th17 cells by segmented filamentous bacteria. *Cell.* 2009;139(3):485-498.
33. Shlomchik WD, Couzens MS, Tang CB, et al. Prevention of graft versus host disease by inactivation of host antigen-presenting cells. *Science.* 1999;285(5426):412-415.
34. Vaishnava S, Behrendt CL, Ismail AS, Eckmann L, Hooper LV. Paneth cells directly sense gut commensals and maintain homeostasis at the intestinal host-microbial interface. *Proc Natl Acad Sci U S A.* 2008; 105(52):20858-20863.
35. Mastroianni JR, Ouellette AJ. Alpha-defensins in enteric innate immunity: functional Paneth cell alpha-defensins in mouse colonic lumen. *J Biol Chem.* 2009;284(41):27848-27856.
36. Hooper LV, Midtvedt T, Gordon JI. How host-microbial interactions shape the nutrient environment of the mammalian intestine. *Annu Rev Nutr.* 2002;22:283-307.
37. Bäckhed F, Ley RE, Sonnenburg JL, Peterson DA, Gordon JI. Host-bacterial mutualism in the human intestine. *Science.* 2005;307(5717):1915-1920.
38. Ley RE, Turnbaugh PJ, Klein S, Gordon JI. Microbial ecology: human gut microbes associated with obesity. *Nature.* 2006;444(7122):1022-1023.
39. Turnbaugh PJ, Ley RE, Mahowald MA, Magrini V, Mardis ER, Gordon JI. An obesity-associated gut microbiome with increased capacity for energy harvest. *Nature.* 2006;444(7122):1027-1031.
40. Manichanh C, Rigottier-Gois L, Bonnaud E, et al. Reduced diversity of faecal microbiota in Crohn's disease revealed by a metagenomic approach. *Gut.* 2006;55(2):205-211.
41. Bollyky PL, Bice JB, Sweet IR, et al. The toll-like receptor signaling molecule Myd88 contributes to pancreatic beta-cell homeostasis in response to injury. *PLoS One.* 2009;4(4):e5063.
42. Penders J, Thijs C, van den Brandt PA, et al. Gut microbiota composition and development of atopic manifestations in infancy: the KOALA Birth Cohort Study. *Gut.* 2007;56(5):661-667.
43. Hill GR, Ferrara JL. The primacy of the gastrointestinal tract as a target organ of acute graft-versus-host disease: rationale for the use of cytokine shields in allogeneic bone marrow transplantation. *Blood.* 2000;95(9):2754-2759.
44. Nestel FP, Price KS, Seemayer TA, Lapp WS. Macrophage priming and lipopolysaccharide-triggered release of tumor necrosis factor alpha during graft-versus-host disease. *J Exp Med.* 1992;175:405-413.
45. Cooke KR, Gerbitz A, Crawford JM, et al. LPS antagonism reduces graft-versus-host disease and preserves graft-versus-leukemia activity after experimental bone marrow transplantation. *J Clin Invest.* 2001;107(12):1581-1589.
46. Gerbitz A, Schultz M, Wilke A, et al. Probiotic effects on experimental graft-versus-host disease: let them eat yogurt. *Blood.* 2004;103(11):4365-4367.
47. Bals R, Wang X, Meegalla RL, et al. Mouse beta-defensin 3 is an inducible antimicrobial peptide expressed in the epithelia of multiple organs. *Infect Immun.* 1999;67(7):3542-3547.
48. Sato T, Vries RG, Snippert HJ, et al. Single Lgr5 stem cells build crypt-villus structures in vitro without a mesenchymal niche. *Nature.* 2009; 459(7244):262-265.

CIN85 is required for Cbl-mediated regulation of antigen receptor signaling in human B cells

Hiroaki Niiro,[1] Siamak Jabbarzadeh-Tabrizi,[1] Yoshikane Kikushige,[2] Takahiro Shima,[1] Kumiko Noda,[1] Shun-ichiro Ota,[1] Hirofumi Tsuzuki,[1] Yasushi Inoue,[1] Yojiro Arinobu,[2] Hiromi Iwasaki,[2] Shinji Shimoda,[1] Eishi Baba,[1] Hiroshi Tsukamoto,[1] Takahiko Horiuchi,[1] Tadayoshi Taniyama,[3] and Koichi Akashi[1]

[1]Department of Medicine and Biosystemic Science, Graduate School of Medical Sciences, Kyushu University, Fukuoka, Japan; [2]Center for Cellular and Molecular Medicine, Kyushu University Hospital, Fukuoka, Japan; and [3]Laboratory of Bacterial Infection and Immunity, Department of Immunology, National Institute of Infectious Diseases, Tokyo, Japan

The aberrant regulation of B-cell receptor (BCR) signaling allows unwanted B cells to persist, thereby potentially leading to autoimmunity and B-cell malignancies. Casitas B-lineage lymphoma (Cbl) proteins suppress BCR signaling; however, the molecular mechanisms that control Cbl function in human B cells remain unclear. Here, we demonstrate that CIN85 (c-Cbl interacting protein of 85 kDa) is constitutively associated with c-Cbl, Cbl-b, and B-cell linker in B cells. Experiments using CIN85-overexpressing and CIN85-knockdown B-cell lines revealed that CIN85 increased c-Cbl phosphorylation and inhibited BCR-induced calcium flux and phosphorylation of Syk and PLCγ2, whereas it did not affect BCR internalization. The Syk phosphorylation in CIN85-overexpressing and CIN85-knockdown cells was inversely correlated with the ubiquitination and degradation of Syk. Moreover, CIN85 knockdown in primary B cells enhanced BCR-induced survival and growth, and increased the expression of BcLxL, A1, cyclin D2, and myc. Following the stimulation of BCR and Toll-like receptor 9, B-cell differentiation-associated molecules were up-regulated in CIN85-knockdown cells. Together, these results suggest that CIN85 is required for Cbl-mediated regulation of BCR signaling and for downstream events such as survival, growth, and differentiation of human B cells. (*Blood.* 2012;119(10):2263-2273)

Introduction

B-cell receptor (BCR) signaling guides critical cell fate decisions in B cells during ontogeny.[1,2] BCRs can generate tolerogenic signals to purge or silence B cells that bind to self-antigens, and immunogenic signals to expand B cells that are specific for foreign antigens. Thus, BCR signaling must be properly regulated at the various stages of B-cell development, as aberrant regulation of BCR signaling potentially leads to autoimmunity and B-cell malignancies.

On BCR ligation by antigens, the Src-family protein tyrosine kinase (PTK) Lyn and Syk are initially activated. Syk propagates the signal by phosphorylating downstream signaling molecules, causing the activation of critical signaling intermediates phosphoinositol 3-kinase (PI3K) and phospholipase C (PLC)γ2. PI3K activates Akt kinase, which is important for B-cell survival.[3] PLCγ2 activation induces the release of intracellular Ca^{2+} and the activation of protein kinase C (PKC), which cause the activation of mitogen-activated protein kinases (MAPKs; ERK, JNK, and p38 MAPK) and of transcription factors, including NF-κB and NF-AT. These molecules regulate further downstream molecules that are responsible for determining B-cell fates such as survival, growth, and differentiation.[1,2]

Casitas B-lineage lymphoma (Cbl) proteins are E3 ubiquitin ligases that regulate signals of various receptors by promoting the ubiquitination of signaling components.[4,5] Tyrosine phosphorylation of Cbl proteins is critical for their function.[6] Mammalian Cbl proteins consist of 3 members, c-Cbl, Cbl-b, and Cbl-3, among which c-Cbl and Cbl-b are expressed in hematopoietic cells.[7] In B cells, Cbl proteins associate with Syk and B-cell linker (BLNK), and negatively regulate BCR signaling.[8,9] B cell-specific ablation of c-Cbl/Cbl-b proteins in mice causes aberrant BCR signaling as well as impaired B-cell anergy, culminating in the development of systemic lupus erythematosus (SLE)–like disease.[10] In addition, c-Cbl is hypophosphorylated on tyrosine in advanced stages of chronic lymphocytic leukemia (CLL).[11] These findings suggest that Cbl-mediated regulation of BCR signaling is critical for the fate decisions of self-reactive and malignant B cells.

Adaptors are noncatalytic molecules that integrate the spatial and temporal assembly of multiprotein complexes involved in the survival, growth, and differentiation of B cells. We previously showed that the B lymphocyte adaptor molecule of 32 kDa (Bam32)/DAPP1 regulates BCR signaling/internalization and B-cell survival.[12,13] The *SH3KBP1* (SH3-domain kinase-binding protein 1) gene, which is also known as CIN85 (c-Cbl interacting protein of 85 kDa), encodes an adaptor that is independently identified by several groups and contains 3 SH3 domains, a proline-rich region, and a coiled-coil domain.[14-17] Early studies showed that in nonimmune cells, CIN85 regulates the clathrin-dependent internalization of receptor tyrosine kinases (RTKs) such as epidermal growth factor receptors (EGFRs).[18,19] The formation of the ternary complex of CIN85, c-Cbl, and endophillin is critical for this process. In immune cells, however, little is known approximately the function of CIN85. CIN85 facilitates ligand-induced FcεRI internalization in RBL-2H3 mast cells.[20] In addition, it regulates FcεRI signaling via Cbl-mediated regulation of

Submitted April 29, 2011; accepted January 13, 2012. Prepublished online as *Blood* First Edition paper, January 18, 2012; DOI 10.1182/blood-2011-04-351965.

The online version of this article contains a data supplement.

The publication costs of this article were defrayed in part by page charge payment. Therefore, and solely to indicate this fact, this article is hereby marked "advertisement" in accordance with 18 USC section 1734.

Syk expression in RBL-2H3 cells.[21] A recent study showed that CIN85 modulates c-Cbl–mediated down-regulation of FcγRIIa in human neutrophils.[22] It is thus of interest to determine whether CIN85 regulates the signaling pathways of other multimeric immune receptors, such as the T- and B-cell receptors.

Here, we demonstrate that CIN85 is constitutively associated with c-Cbl, Cbl-b, and BLNK in human B cells. Gain-of-function and loss-of-function experiments revealed that CIN85 up-regulated c-Cbl phosphorylation and inhibited BCR-induced calcium flux and phosphorylation of Syk and PLCγ2, without affecting BCR internalization. CIN85 also promoted c-Cbl–dependent ubiquitination and degradation of Syk. Moreover, CIN85 knockdown in primary B cells caused enhanced BCR-induced survival and growth, and augmented BCR/TLR9-induced expression of B-cell differentiation-associated molecules. Collectively, these results suggest that CIN85 is required for Cbl-mediated regulation of BCR signaling and for downstream events such as the survival, growth, and differentiation of human B cells.

Methods

Reagents

Goat anti–human IgM and IgG/IgA/IgM F(ab′)$_2$ fragments were purchased from Jackson ImmunoResearch Laboratories. Rabbit anti–human phospho-Zap-70 (Y319)/Syk (Y352), anti–human phospho-PLCγ2 (Y1217), anti–human phospho-Akt, anti–mouse Akt, anti–human phospho-JNK, anti–human phospho-ERK, and anti–human PLCγ2 pAbs as well as anti–human BclxL and Blimp-1 mAbs were purchased from Cell Signaling Technology. Mouse anti–human phospho-Btk, anti–human phospho-BLNK, anti–human c-Cbl, and anti–human Rac1 mAbs were from BD Immunocytometry. Mouse anti–human Cbl-b, anti–human Syk (4D10), anti–human BLNK, and anti-ubiquitin mAbs as well as rabbit anti–human c-Cbl and anti–mouse cyclin D2 pAbs were from Santa Cruz Biotechnology. Mouse anti-V5 mAb was from Invitrogen. Mouse anti-phosphotyrosine and anti–human CIN85 mAbs were from Upstate Biotechnology. Rabbit anti–human Vav2 mAb was from Epitomics. Sheep anti–human CD2AP pAb was from R&D Systems. Mouse anti–β-actin mAb was from Sigma-Aldrich.

B cell lines and primary B cells

The B lymphoma cell line BJAB was cultured in RPMI 1640 medium supplemented with 10% FCS. Human peripheral blood mononuclear cells, kindly provided by healthy volunteers, were separated from their buffy coats. Informed consent was obtained from all subjects in accordance with the Declaration of Helsinki. The Institutional Review Board of Kyushu University Hospital approved all research on human subjects. B cells were isolated with Dynabeads M450 CD19 and DETACHaBEAD CD19 (Dynal Biotech), according to the manufacturer's instructions. The isolated B cells exhibited greater than 99.5% viability on trypan blue exclusion and more than 95% purity on flow cytometry. Trace levels of phosphorylation of BCR-signaling molecules were observed in the B cells immediately after purification, probably because of mechanical stress.[23] The cells were thus rested for a couple of hours before further analysis. The cells were cultured at a density of 1×10^6 cells/mL in a 96 flat-bottom microtiter plate in complete RPMI 1640 medium supplemented with 10% FCS.

Expression constructs and transfection

Constructs encoding V5-tagged wild-type (WT) and 3 SH3 domain-deleted mutants of human CIN85 (pEF1/V5-CIN85 and –CIN85-dSH3ABC) were previously described.[24] The BJAB cells were transfected with the aforementioned constructs using a Gene Pulser apparatus (Bio-Rad Laboratories). The control cells were transfected with an empty vector. Stably transfected BJAB clones were selected in the presence of G418 (2 mg/mL) and screened with anti-V5 mAb.

RNA interference

The pSUPER-based strategy was adopted to knockdown hCIN85 expression. To generate CIN85 small-hairpin RNA (shRNA), a 19-nucleotide sequence (CAGCAATGACATTGACTTA) selected from human CIN85 cDNA was annealed and ligated into the pSUPER or GFP-pSUPER vector. A scrambled sequence (GTTACTAACGCGAATTAAC) was used as negative control. hCIN85 or the control shRNA vector was transfected into BJAB cells using a Gene Pulser apparatus, and stable hCIN85-knockdown BJAB clones were selected in the presence of puromycin (0.5 μg/mL). Transient transfections of primary B cells with the pSUPER-hCIN85 vector were performed using the Nucleofection kit from AMAXA Biosystems as previously described.[23]

Measurement of intracellular free calcium

B cells were washed with RPMI 1640 medium containing 10% FCS and adjusted to a concentration of 1×10^6 cells/mL. After incubation at 37°C for 15 minutes, 1 μg/mL of Fluo 4/AM (Dojindo) was added, and the cells were incubated for an additional 30 to 45 minutes with resuspension every 15 minutes. The cells were centrifuged and resuspended in RPMI 1640 at a density of 2×10^6 cells/mL and stimulated with anti-IgM (20 μg/mL). The fluorescence intensity of intracellular Fluo 4 was monitored and analyzed using flow cytometry.

Immunoprecipitation

Cells were lysed as described.[13] Subsequently, protein G-Sepharose (Amersham Pharmacia Biotech) precleared lysates were incubated with anti-V5, -BLNK, -Syk, -Cbl, -Vav2 mAb, or -CD2AP pAb for 1 hour at 4°C and then immunoprecipitated with protein G-Sepharose overnight at 4°C. The precipitated proteins were resolved by 10% SDS-PAGE; transferred onto a Millipore Immobilon polyvinylidene difluoride membrane; and blotted with anti-phosphotyrosine (4G10), -V5, -c-Cbl, -Cbl-b, -BLNK, -Vav2, -Syk, or -ubiquitin mAbs, followed by incubation with secondary HRP-conjugated IgG (Jackson ImmunoResearch Laboratories) specific for the primary Ab. The blots were developed with an ECL Plus kit (Amersham Biosciences).

Western blot analysis

Nonstimulated or stimulated cells (1×10^6) were lysed as described.[12] The lysates were then denatured in an equal volume of 2 × SDS sample buffer, resolved on a 10% SDS-PAGE gel, and electro-transferred to nitrocellulose membranes in non-SDS–containing transfer buffer (25mM Tris, 0.2M glycine, and 20% methanol; pH 8.5). Western blotting was performed with anti–phospho-Syk (1:2000), anti–phospho-PLCγ2 (1:2000), anti–phospho-BLNK (1:2000), anti–phospho-JNK (1:2000), anti–phospho-ERK (1:2000), anti–phospho-Akt (1:2000), anti-Akt (1:2000), anti-CIN85 (1:2000), anti–β-actin (1:2000), or anti-Vav2 (1:2000), followed by a 1:15 000 dilution of anti–rabbit or anti–mouse HRP-conjugated IgG. The blots were developed with the ECL plus kit (Amersham Biosciences). The chemiluminescence intensity was monitored using a Laser3000 (FujiFilm) instrument. We quantitated the band intensity of the proteins using ImageGauge Version 4.22 software (FujiFilm). The resulting values were expressed as fold changes in protein expression relative to the protein expression in unstimulated control cells.

Luciferase assays

Cells (1×10^7) were transfected by electroporation with the NF-AT-reporter construct, which was generously provided by Dr Shoichiro Miyatake (The Tokyo Metropolitan Institute of Medical Science, Tokyo, Japan). After 18 to 20 hours, cells were harvested and plated on 96-well plates at a density of 2×10^5/well. Triplicate cultures were incubated in the media alone with graded doses of anti-IgM or with 50nM PMA and 2.5μM ionomycin. After 6 hours, the cells were lysed in 50 μL reporter lysis buffer (Promega) for 15 minutes at room temperature. The luciferase activity was assayed by adding 20 μL luciferase substrate (Promega) to 50 μL lysate

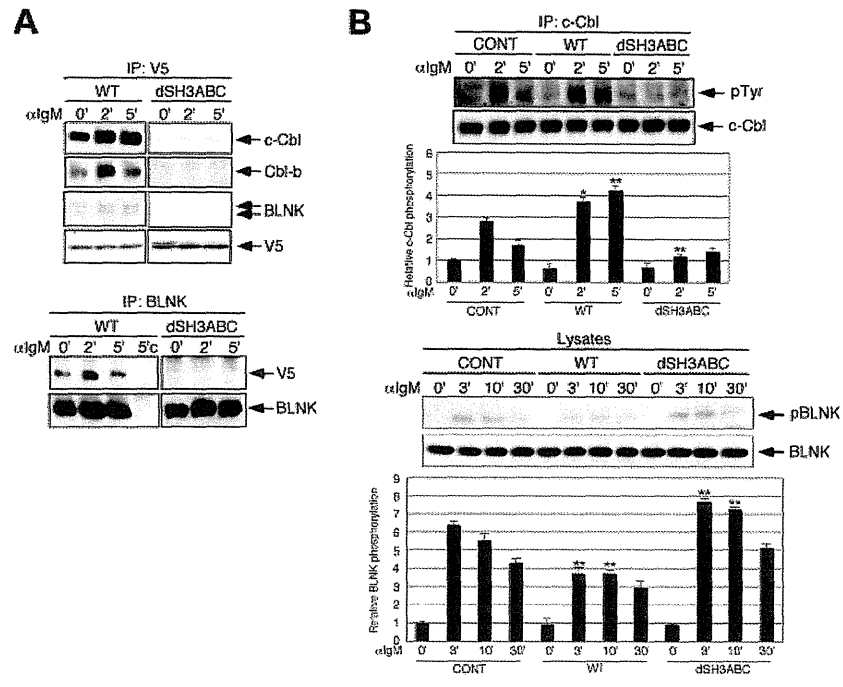

Figure 1. CIN85 associates with Cbl and BLNK and regulates their phosphorylation in B cells. (A) BJAB cells stably expressing either WT or SH3-deleted CIN85 were stimulated with 20 μg/mL of F(ab′)$_2$ goat anti–human IgM for the indicated time periods. Immunoprecipitates with anti-V5 or anti-BLNK mAb were separated on a 10% SDS-PAGE gel and analyzed by Western blotting with anti–c-Cbl, anti–Cbl-b, anti-BLNK, or anti-V5 mAb. 5′c, immunoprecipitation of the cell lysates at 5 minutes with isotype control. (B) Control BJAB cells and stable transformants expressing either WT or SH3-deleted CIN85 were stimulated with 20 μg/mL of F(ab′)$_2$ goat anti–human IgM for the indicated time periods. Immunoprecipitates with anti–c-Cbl mAb were separated on a 10% SDS-PAGE gel and analyzed by Western blotting with anti-phosphotyrosine or anti–c-Cbl mAb. The resulting values are expressed as fold changes in protein expression compared with unstimulated control cells. The values are the mean ± SD of 3 independent experiments (*$P < .05$, **$P < .01$ vs controls). (C) Control BJAB cells and stable transformants expressing either WT or SH3-deleted CIN85 were stimulated with 20 μg/mL of F(ab′)$_2$ goat anti–human IgM for the indicated time periods. The cell lysates were subsequently separated on a 10% SDS-PAGE gel and analyzed by Western blotting with anti–phospho-BLNK or anti-BLNK mAb. The resulting values are expressed as fold changes in protein expression compared with unstimulated control cells. The values are the mean ± SD of 3 independent experiments (**$P < .01$ vs controls).

and immediately measuring the luminescence on a Lumat LB9507 luminometer (EG & G Berthold). To serve as a control for the transfection efficiency, the relative luciferase activity of the medium and cells stimulated with BCR was calculated relative to stimulation with PMA/ionomycin.

Flow cytometric analysis

BJAB cells were incubated on ice for 15 minutes with 20 μg/mL goat-unlabeled anti-IgM before they were washed with ice-cold medium and warmed at 37°C for the indicated time intervals. The cells were washed with ice-cold PBS containing 2% FBS and 0.2% sodium azide (Fisher Scientific) to stop internalization at the assigned time points and to remove the unbound Ab. The remaining surface BCRs were stained with FITC-labeled rabbit anti–goat Ig and quantified by flow cytometry. The data are presented as the percentage of surface BCR remaining.

Fluorescence microscopic analysis

BJAB cells were incubated with 10 μg/mL of unlabeled goat anti–human IgM sera (20 μg/mL) at 4°C for 30 minutes and warmed to 37°C for the indicated time periods. The cells were then fixed with 3.7% paraformaldehyde and permeabilized with PBS containing 1% BSA and 0.05% saponin (wash buffer). The cells were then incubated for 30 minutes with FITC-conjugated anti–goat IgG pAb (Jackson ImmunoResearch Laboratories) at 4°C. The stained cells were centrifuged onto slides and analyzed with inverted fluorescent microscopy (BZ-9000; Keyence).

Quantitative real-time PCR

The total RNA was extracted from the primary B cells using Isogen reagent (Nippon gene) and was treated with DNase I (Invitrogen) to remove contaminating genomic DNA. First-strand cDNA was synthesized using a QuantiTect reverse transcription kit (QIAGEN). Quantitative real-time PCR was performed in the ABI Prism 7700 Sequence Detector (Applied Biosystems). The reactions were performed in triplicate wells in 96-well plates. TaqMan target mixes for Cyclin D2, Myc, *BCL2L1*/BclxL, *BCL2A1*/A1, *PRDM1*/Blimp-1, and *XBP1* were purchased from Applied Biosystems. 18S ribosomal RNA (rRNA) was separately amplified in the same plate as an internal control for variation in the amount of cDNA in PCR. The collected data were analyzed using the Sequence Detector software (Applied Biosystems). The data were expressed as the fold change in gene expression relative to the expression in the control cells.

Annexin V staining

After culture, cells (1-2 × 10^5) were washed twice with PBS and suspended in 85 μL binding buffer (MBL) containing Ca^{2+}. The cell suspension supplemented with 10 μL annexin-V–FITC or annexin-V–PE (MBL) and 5 μg of propidium iodide (PI) or 1 μg of 7-ADD was incubated at room temperature for 15 minutes in the dark. Subsequently, binding buffer was added, and the fraction of early apoptotic cells was measured using flow cytometry.

BrdU assay

DNA synthesis was monitored by pulse-labeling cells for 2 hours with the thymidine analog 5-bromo-2′-deoxyuridine (BrdU). The cells were washed 3 times with PBS and fixed for 20 minutes at −20°C in an ethanol fixative (0.15mM glycine in 70% EtOH, pH 2.0). After rehydration in PBS, BrdU incorporation was detected by incubation with an anti-BrdU mAb for 1 hour at 37°C, followed by a rhodamine-conjugated anti–mouse antibody (1:500; Jackson ImmunoResearch Laboratories) and staining of the nucleus with 4′-6-diamidino-2-phenylindole for 1 hour. The proportion of BrdU-positive nuclei (BrdU labeling index) was assessed, based on a sample size of 500 cells per data point.

Statistical analysis

Statistical analysis was performed using the Student t test. $P < .05$ was considered statistically significant.

Results

CIN85 associates with Cbl and BLNK and regulates their phosphorylation

The tyrosine phosphorylation of signaling molecules is a critical event in BCR signaling.[1,2] Because SH3 domains play an important role in the function of CIN85,[25] we focused on

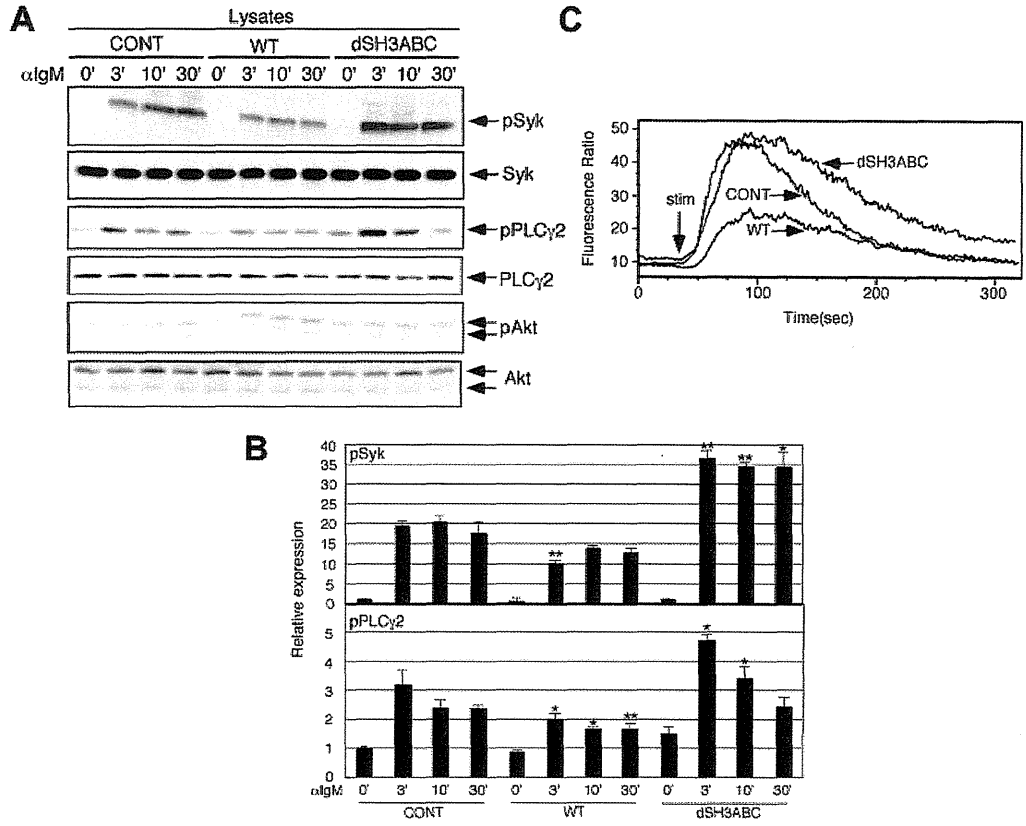

Figure 2. Forced CIN85 expression inhibits BCR-induced calcium flux and phosphorylation of Syk and PLCγ2. (A-B) Control BJAB cells and stable transformants expressing either WT or SH3-deleted CIN85 were stimulated with 20 μg/mL of $F(ab')_2$ goat anti–human IgM for the indicated time periods. The cell lysates were subsequently separated on a 10% SDS-PAGE gel and analyzed by Western blotting with anti–phospho-Syk pAb, anti-Syk mAb, anti–phospho-PLCγ2 pAb, anti-PLCγ2 pAb, anti–phospho-Akt pAb, or anti-Akt pAb. The resulting values are expressed as fold changes in protein expression compared with unstimulated control cells. The values are the mean ± SD of 3 independent experiments (*$P < .05$, **$P < .01$ vs controls). (C) Ca^{2+} influx in control BJAB cells and stable transformants expressing either WT or SH3-deleted CIN85. The intracellular free calcium levels in Fluo 4/AM-loaded cells were analyzed using flow cytometry after the cells were stimulated with 20 μg/mL $F(ab')_2$ goat anti–human IgM. The results shown are representative of 4 independent experiments.

tyrosine-phosphorylated molecules downstream of the BCR that could associate with the SH3 domains of CIN85. Specifically, we focused on the 2 molecules, BLNK and c-Cbl, that function as key positive and negative regulators of BCR signaling,[1,10] respectively; both proteins can associate with the SH3 domains of CIN85.[14,26]

We first determined the association of Cbl and BLNK with CIN85 using WT and SH3-deleted CIN85-expressing B cell lines. Consistent with previous reports,[14,26] WT CIN85 was constitutively associated with c-Cbl and BLNK, and these associations were increased after BCR stimulation (Figure 1A). Cbl-b was similarly associated with WT CIN85, albeit to a lesser extent. Although the association of WT CIN85 and BLNK appeared modest, the inverse immunoprecipitation of BLNK confirmed the association (Figure 1A). As expected, the association of Cbl and BLNK with CIN85 was abrogated in SH3-deleted CIN85-expressing B cells, suggesting that the SH3 domains of CIN85 are required for its association with Cbl and BLNK. Because the tyrosine phosphorylation of c-Cbl and BLNK is critical for their function,[6,27] we next determined whether the overexpression of WT and SH3-deleted CIN85 affects BCR-induced phosphorylation of c-Cbl and BLNK. Compared with control cells, WT and SH3-deleted CIN85 sustained and inhibited c-Cbl phosphorylation, respectively (Figure 1B). In addition, WT and SH3-deleted CIN85 inhibited and enhanced BLNK phosphorylation, respectively (Figure 1B). These findings suggest that CIN85 associates with Cbl and BLNK and regulates their phosphorylation in an opposite manner.

Forced CIN85 expression inhibits BCR-induced calcium flux and the phosphorylation of Syk and PLCγ2

We tested whether the overexpression of WT and SH3-deleted CIN85 affects early BCR signaling. Syk phosphorylation, which is one of the earliest events in BCR signaling, was inhibited in WT CIN85-expressing cells, whereas it was sustained in SH3-deleted CIN85-expressing cells (Figure 2A-B). Two enzymes, PLCγ2 and PI3K, function as critical mediators downstream of BCR signaling.[1,2,28] WT and SH3-deleted CIN85 partially inhibited and enhanced BCR-induced phosphorylation of PLCγ2, respectively (Figure 2A-B). In contrast, the phosphorylation of Akt, which is a downstream molecule of PI3K, was not affected in WT or SH3-deleted CIN85-expressing cells (Figure 2A). Activated PLCγ2 converts PIP2 into IP3 and diacyl glycerol, of which PIP2 is critical for calcium flux in B cells.[1,2,12] Consistent with the levels of PLCγ2 phosphorylation, the BCR-induced calcium flux was significantly inhibited in WT CIN85-expressing cells, whereas it was slightly sustained in SH3-deleted CIN85-expressing cells (Figure 2C). These results suggest that CIN85 inhibits BCR-induced calcium flux and the

phosphorylation of Syk and PLCγ2, and that the SH3 domains of CIN85 are required for its inhibitory function.

CIN85 knockdown enhances BCR-induced calcium flux and the phosphorylation of Syk, Vav2, and PLCγ2, leading to augmented NF-AT activation and CD69 expression

To elucidate the role of endogenously expressed CIN85 in BCR signaling, we generated CIN85-knockdown B cell lines. In contrast to the CIN85-overexpressing cells (Figures 1 and 2), CIN85-knockdown cells exhibited enhanced phosphorylation of Syk, BLNK, and PLCγ2 (Figure 3A-B). Akt phosphorylation was comparable between control and CIN85-knockdown cells (Figure 3A). Consistent with the levels of PLCγ2 phosphorylation, BCR-induced calcium flux was accentuated in CIN85-knockdown cells (Figure 3C). Vav2 positively regulates PLCγ2 activation in B cells.[29] Vav2 phosphorylation was enhanced in CIN85-knockdown cells (Figure 3D). These BCR signaling profiles in CIN85-knockdown cells are reminiscent of those in c-Cbl/Cbl-b double-knockout B cells.[10] The phosphorylation of c-Cbl was significantly inhibited in CIN85-knockdown cells (Figure 3E). BCR-induced calcium flux plays a crucial role in the activation of the transcription factor NF-AT, the disruption of which results in significant defects in B-cell function.[30] BCR-induced NF-AT activation was enhanced in CIN85-knockdown cells (Figure 3F). In addition, BCR-induced up-regulation of the activation marker CD69 was pronounced in CIN85-knockdown cells (Figure 3G). These phenotypes in CIN85-knockdown cells were again similar to those observed in Cbl-deficient B cells.[10] Given that CIN85 strongly associates with Cbl proteins (Figure 1A), these results suggest that CIN85 plays a vital role in Cbl-mediated regulation of BCR signaling.

CIN85 promotes the ubiquitination and degradation of Syk in B cells

Cbl proteins function as E3 ubiquitin ligases and target PTK substrates, including Syk, for degradation.[31,32] We thus tested whether CIN85 affects Syk ubiquitination in B cells. Syk ubiquitination was induced on BCR stimulation. Compared with control cells, Syk ubiquitination was increased in WT CIN85-expressing cells (Figure 4A). In contrast, an impairment in Syk ubiquitination was noted in CIN85-knockdown cells (Figure 4A). These results suggest that CIN85 positively regulates Cbl-mediated ubiquitination of BCR-signaling molecules including Syk. Despite the altered levels of Syk ubiquitination, the level of total Syk protein was not altered in the WT CIN85-expressing or CIN85-knockdown cells throughout the stimulation (Figures 2A and 3A). Because only a small pool of Syk is phosphorylated on stimulation and targeted for degradation in B cells,[31] we tested the degree of Syk phosphorylation among the total Syk immunoprecipitate. The levels of phosphorylated Syk were reduced in WT CIN85-expressing cells but enhanced in CIN85-knockdown cells (Figure 4B), suggesting that CIN85 promotes Cbl-dependent loss of the phosphorylated pool of Syk in B cells.

CIN85 does not affect BCR internalization

CIN85 regulates Cbl-mediated internalization of the EGFR in several cell types other than B cells.[18,19] To test whether CIN85 affects BCR internalization, we first monitored the levels of surface BCR expression after stimulation. Without stimuli, the levels of surface BCR were similar on CIN85 overexpression and CIN85 knockdown. In parental cells, BCR crosslinking caused a rapid decrease in surface BCR levels, suggesting that BCR was efficiently internalized after stimulation (Figure 5A; supplemental Figure 1A, available on the *Blood* Web site; see the Supplemental Materials link at the top of the online article). BCR internalization was not affected in the WT or SH3-deleted CIN85-expressing cells. Moreover, the absence of endogenous CIN85 did not affect BCR internalization (Figure 5B, supplemental Figure 1A). Next, we directly visualized BCRs in B cell lines using fluorescence microscopy. In control cells, the BCR complexes exhibited a slightly patchy distribution before stimulation, and within 3 minutes after stimulation, the BCRs formed polarized tight caps on the cell surface. After 10 minutes of BCR stimulation, a punctate pattern of internalized BCRs was clearly visualized (Figure 5C). Consistent with the findings obtained with flow cytometry (Figure 5A-B), the spatial and temporal distribution of BCR complexes in CIN85-overexpressing and CIN85-knockdown cells appeared similar to that in control cells (Figure 5C, supplemental Figure 1B-C). These findings suggest that CIN85 does not affect BCR internalization.

CIN85 knockdown enhances the survival, growth, and differentiation of primary B cells

BCR signaling plays a critical role in determining the survival, growth, and differentiation of B cells.[1] It was thus of interest to test whether CIN85 affects B cell fate. A major obstacle, however, is that the survival, growth, and differentiation of B cell cannot be properly assessed in transformed B cells. We therefore sought to knock down CIN85 expression in human primary B cells. After introduction of the GFP-CIN85 knockdown vector, GFP-positive B cells were sorted and used for further experimentation. Under these conditions, we were able to knock down the CIN85 mRNA expression in B cells by 60%-80% (Figure 6A).

We first tested whether CIN85 knockdown affects the expression of the B-cell survival-associated genes BcLxL and A1. Consistent with previous studies,[33] BCR stimulation induced BcLxL and A1 mRNA expression in control cells. This induction was far more drastic in CIN85-knockdown B cells (Figure 6A). The costimulation of TLR9 with its ligand CpG enhances BCR-induced expression of B-cell survival genes.[34] This enhancement was less evident in CIN85-knockdown cells than in control cells (Figure 6A), suggesting that CIN85 knockdown requires less costimulation for the full induction of B-cell survival genes. Consistent the findings for the transcript levels, the BCR-induced expression of BcLxL protein was more pronounced in CIN85-knockdown cells (Figure 6B). We also tested whether CIN85 knockdown affects BCR-induced death of B cells using the annexin-binding assay. The CIN85-knockdown cells exhibited less BCR-induced cell death (Figure 6C). We next tested whether CIN85 knockdown affects the expression of the B-cell growth-associated genes cyclin D2 and myc. Again, BCR-induced expression of these genes was more pronounced in CIN85-knockdown cells (Figure 6A), and costimulation with TLR9 did not enhance induction compared with the control cells. Consistent with the findings for the transcript levels, BCR-induced expression of cyclin D2 protein was more pronounced in CIN85-knockdown cells (Figure 6B). We also tested whether CIN85 knockdown affects B-cell growth using the BrdU uptake assay. Consistent with the expression levels of cyclin D2 and myc, CIN85 knockdown enhanced BCR-induced cell growth (Figure 6D). On activation, B cells undergo plasma cell differentiation along with the expression of critical differentiation-associated genes such as Blimp-1 and Xbp-1. Consistent with previous studies,[35] BCR stimulation alone was not sufficient to induce the expression of Blimp-1 and Xbp-1 in human B cells (data not shown). However, the combined stimulation of BCR and TLR9 clearly induced the expression of these genes in control cells,

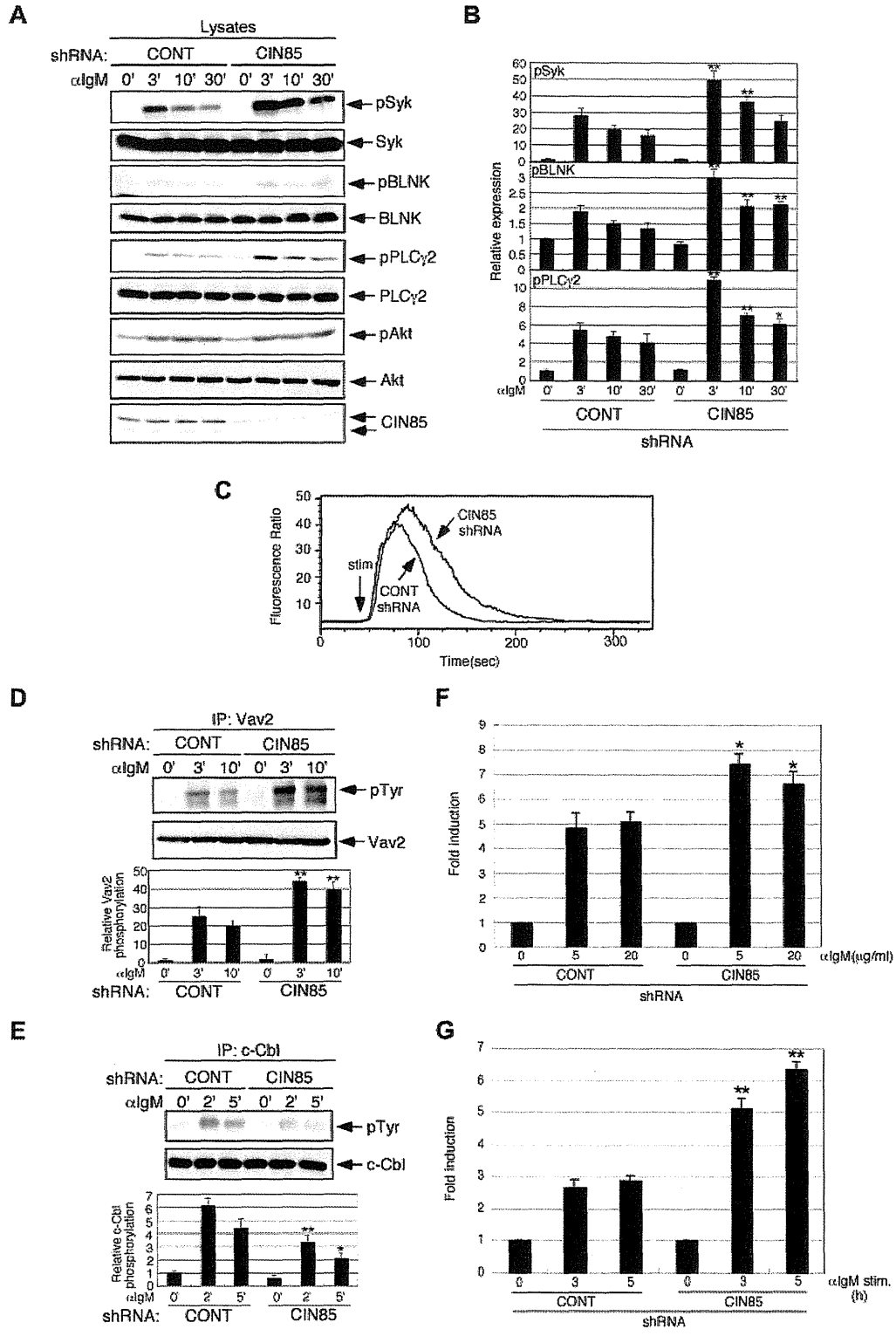

Figure 3. CIN85 knockdown enhances BCR-induced calcium flux and phosphorylation of Syk, Vav2, and PLCγ2, leading to augmented NF-AT activation and CD69 expression. (A-B) Stable control and CIN85-knockdown BJAB cells were stimulated with 20 μg/mL F(ab′) $_2$ goat anti–human IgM for the indicated time periods. The cell lysates were subsequently separated on a 10% SDS-PAGE gel and analyzed by Western blotting with anti–phospho-Syk pAb, anti-Syk mAb, anti–phospho-BLNK mAb, anti-BLNK mAb, anti–phospho-PLCγ2 pAb, anti-PLCγ2 pAb, anti–phospho-Akt pAb, anti-Akt pAb, or anti-CIN85 mAb. The resulting values are expressed as fold changes in protein expression compared with unstimulated control cells. The values are the mean ± SD of 3 independent experiments (*$P < .05$, **$P < .01$ vs controls). (C) Ca^{2+} influx in stable control and CIN85-knockdown BJAB cells. Intracellular free calcium levels in Fluo 4/AM-loaded cells were analyzed using flow cytometry after the cells were stimulated with 20 μg/mL F(ab′)$_2$ goat anti–human IgM. The results shown are representative of 4 independent experiments. (D-E) Stable control and CIN85-knockdown BJAB cells were stimulated with 20 μg/mL F(ab′)$_2$ goat anti–human IgM for the indicated time periods. Immunoprecipitates with anti-Vav2 or anti–c-Cbl mAb were separated on a 10% SDS-PAGE gel and analyzed by Western blotting with anti-phosphotyrosine mAb, anti-Vav2 mAb, or anti–c-Cbl mAb. The resulting values are expressed as fold changes in protein expression compared with unstimulated control cells. The values are the mean ± SD of 3 independent experiments (*$P < .05$, **$P < .01$ vs controls). (F) Stable control

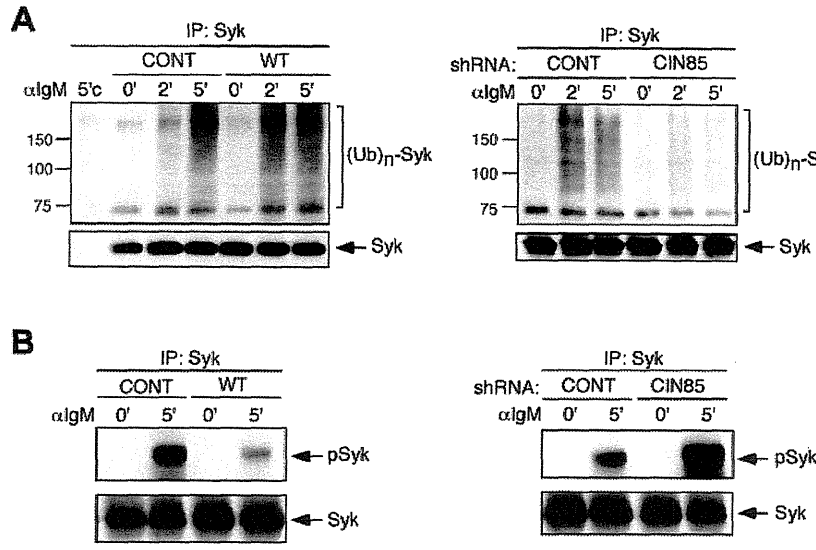

Figure 4. CIN85 promotes Syk ubiquitination and degradation in B cells. (A) Control BJAB cells, stable transformants expressing WT CIN85, and CIN85-knockdown BJAB cells were stimulated with 20 μg/mL $F(ab')_2$ goat anti–human IgM for the indicated time periods. Immunoprecipitates with anti-Syk mAb were separated on a 10% SDS-PAGE gel and analyzed by Western blotting with anti-ubiquitin or anti-Syk mAb. 5"c, immunoprecipitation of the cell lysates at 5 minutes with isotype control. The molecular weight is indicated on the left side of the blots. (B) Control BJAB cells, stable transformants expressing WT CIN85, and CIN85-knockdown BJAB cells were stimulated with 20 μg/mL $F(ab')_2$ goat anti–human IgM for 5 minutes. Immunoprecipitates with anti-Syk mAb were separated on a 10% SDS-PAGE gel and analyzed by Western blotting with anti–phospho-Syk pAb or anti-Syk mAb.

whereas this induction was more pronounced in CIN85-knockdown B cells (Figure 6E). Consistent with the findings for the transcript levels, BCR stimulation alone did not induce detectable levels of Blimp-1 protein. However, the combined stimulation of BCR and TLR9 clearly induced the expression of the Blimp-1 protein in control cells, although this was more pronounced in CIN85-knockdown cells (Figure 6F). These results suggest that CIN85 is required for Cbl-mediated regulation of BCR signaling and downstream events such as the survival, growth, and differentiation of human B cells.

Discussion

We demonstrated here that CIN85 functions as a novel adaptor to regulate proximal BCR signaling. Gain-of-function and loss-of-function experiments revealed that CIN85 not only enhances BCR-induced c-Cbl phosphorylation but also inhibits BCR-induced calcium flux and the phosphorylation of Syk and PLCγ2. CIN85 promotes c-Cbl–dependent ubiquitination and degradation of Syk, which is a key upstream kinase that propagates BCR signaling by phosphorylating downstream molecules including PLCγ2. Because Cbl proteins directly associate with Syk and inhibit its function,[6] it is probable that CIN85 acts as a critical scaffolding adaptor for Cbl proteins and is indispensable for Cbl-mediated regulation of Syk activation in B cells.

Consistent with our findings, a critical role of CIN85 in Cbl-mediated regulation of Syk activation was recently shown in FcεRI signaling in mast cells.[21] In mast cells, CIN85 enhances c-Cbl-mediated ubiquitination and the degradation of Syk protein.[21] In B cells, however, CIN85 overexpression significantly increased Syk ubiquitination (Figure 4), but CIN85 knockdown did not alter the total levels of Syk protein throughout stimulation (Figure 3A), as previously shown in c-Cbl/Cbl-b double-knockout B cells.[10] This apparent discrepancy in Syk degradation between mast cells and B cells could be explained by the findings of Rao et al,[31] who showed that on BCR stimulation, only a small portion of Syk is phosphorylated and then degraded by c-Cbl. Rao et al also showed that c-Cbl does not directly affect the catalytic activity of Syk.[31] Consistent with these findings, our study showed that CIN85 promotes c-Cbl–mediated ubiquitination and degradation of the phosphorylated pool of Syk (Figure 4A-B).

What, then, are the possible mechanisms by which CIN85 enhances BCR-induced c-Cbl phosphorylation in B cells? Src-family PTKs and Syk are proposed to phosphorylate c-Cbl on tyrosines.[6] We previously showed that CIN85 directly interacts with the SH3 domain of Src-family PTKs including Lyn.[17] In addition, CIN85 directly associates with BLNK, PLCγ and Vav, all of which are direct Syk interactors,[17,36] and thus, CIN85 is indirectly associated with Syk via binding to BLNK, PLCγ, and Vav. In view of these findings, it seems probable that CIN85 acts as a key scaffolding adaptor that permits the spatial proximity of Src-family PTKs, Syk, and Cbl proteins and thus facilitates their phosphorylation of Cbl proteins.

Although CIN85 appears to function in concert with Cbl proteins to regulate BCR signaling, an additional mechanism is possible. Previous in vitro binding experiments showed that CIN85 directly binds to Src-family tyrosine kinases, PLCγ, p85 PI3K, Vav, Btk, and SHIP, all of which are involved in BCR signaling, through its SH3 domains and proline-rich region.[15,24,25] In addition, a recent study showed that the SH3 domains of CIN85 could uniquely bind to ubiquitin.[37] Thus, after various BCR-signaling molecules are ubiquitinated by Cbl proteins on stimulation, the competition between canonical SH3 ligands and ubiquitin binding to CIN85 may affect BCR signaling in a temporal and spatial manner. Therefore, it is probable that CIN85 also directly regulates BCR signaling by a Cbl-independent mechanism.

A recent study using liquid chromatography-coupled tandem mass spectrometry showed that 3 SH3 domains of CIN85 could recruit protein molecules required for the proper formation and

Figure 3 (continued) and CIN85-knockdown BJAB cells transfected with the NF-AT luciferase reporter construct were stimulated with graded doses of $F(ab')_2$ goat anti–human IgM for 8 hours and lysed, and the luciferase activity was assayed using a luminometer. The relative luciferase activity of the medium and BCR-stimulated cells was expressed with respect to that of the PMA/ionomycin stimulation. The results were presented as the mean and SEM of triplicate cultures. One experiment representative of 4 independent experiments is shown (*$P < .05$ vs controls). (G) Stable control and CIN85-knockdown BJAB cells before and after stimulation with 20 μg/mL $F(ab')_2$ goat anti–human IgM (3 and 5 hours) were analyzed for surface expression of CD69. One experiment representative of 3 independent experiments is shown (**$P < .01$ vs controls).

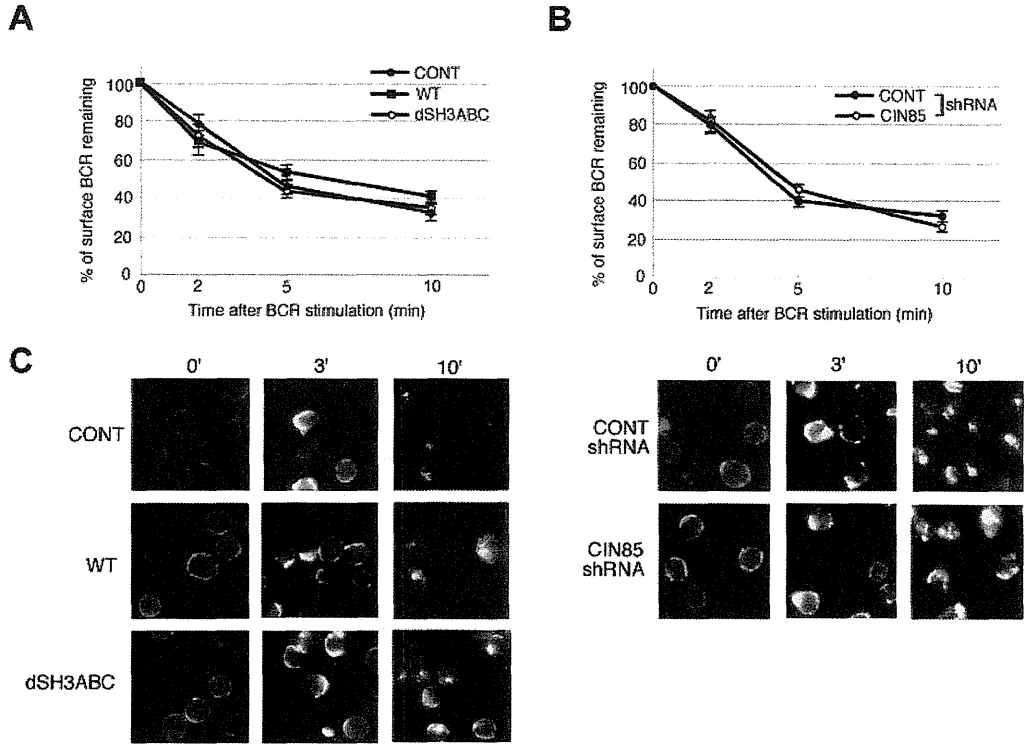

Figure 5. CIN85 does not affect BCR internalization. (A) BJAB cells (control and stable transformants expressing either WT or SH3-deleted CIN85) and (B) BJAB cells (control and CIN85-knockdown) were incubated at 4°C with $F(ab')_2$ goat anti–human IgM for 30 minutes. The cells were washed, warmed to 37°C for the indicated time intervals, stained at 4°C for 30 minutes with a FITC-labeled anti–goat IgG pAb, and analyzed by flow cytometry. The results are expressed as the percentage of surface BCRs remaining. The data are presented as the average and SEM of 3 independent experiments. (C) Control BJAB cells, stable transformants expressing either WT or SH3-deleted CIN85, and CIN85-knockdown BJAB cells were incubated at 4°C with 20 μg/mL $F(ab')_2$ goat anti–human IgM for 30 minutes. The cells were washed and warmed to 37°C for the indicated time periods. The cells were fixed, permeabilized, stained with a FITC-labeled anti–goat IgG pAb, and analyzed by fluorescence microscopy. The images shown are representative of 3 independent experiments.

function of coated vesicles.[25] Similarly, early studies showed a characteristic feature of CIN85 in the formation of clathrin-coated vesicles during the internalization of RTKs such as EGFRs in nonimmune cells.[18,19] Brain-specific CIN85-deficient mice manifest impaired internalization of D2 dopamine receptors, which belong to the 7-transmembrane G protein-coupled receptor superfamily.[38] In addition, CIN85 facilitates ligand-induced FcεRI internalization in RBL-2H3 mast cell lines.[20] Because BCR internalization is regulated via a clathrin-dependent pathway,[39] it was of interest to determine whether CIN85 regulates BCR internalization. Our study, however, shows that CIN85 does not affect BCR internalization (Figure 5, supplemental Figure 1). These data are somewhat surprising, given that Cbl proteins control BCR internalization by a ubiquitin-dependent mechanism.[10,40] However, the role of Cbl proteins in BCR ubiquitination and internalization is still rather controversial. The HECT family member Itch, but not c-Cbl, is an E3 ubiquitin ligase that is involved in BCR ubiquitination.[41] In addition, the ubiquitination of Igβ, which is a component of BCR, does not facilitate BCR internalization but is required for the sorting of early endosomes and for trafficking into late endosomes,[41] which suggests that BCR ubiquitination is more critical at the later stage of its trafficking. Because our imaging analysis (Figure 5C) cannot clearly distinguish the spatial distribution of early and late endosomes, it is of great interest to test whether CIN85 affects postendocytotic BCR trafficking. A recent study showed that in human neutrophils, CIN85 modulates c-Cbl–mediated down-regulation of FcγRIIa in the later stages of receptor trafficking without affecting the internalization of this receptor.[22]

During the submission of this paper, 2 studies were published that, in contrast to our findings, showed that CIN85 positively regulates BCR signaling in mouse and chicken B cells.[42,43] These studies found that CIN85 associates with BLNK and regulates BCR-induced NF-κB activation. However, the detailed profiles of BCR signaling differ between the 2 studies: the BCR-induced phosphorylation of BLNK and PLCγ2 and the calcium flux are significantly decreased on the loss of CIN85 in chicken B cells, whereas they are apparently normal in CIN85-deficient mouse B cells.[42,43] It should be noted that the former study did not actually use CIN85-deficient cells; rather, it used cells expressing a mutant BLNK that failed to bind to CIN85 or its homolog CD2AP.[42] Although these findings are intriguing, it is rather surprising that Cbl-mediated function of CIN85 in B cells was barely investigated in these studies. As previously mentioned, it is becoming evident that Cbl proteins play a critical role in the function of CIN85 in immune cells.[20-22] In addition, BCR-induced association of CIN85 with c-Cbl was recently shown even in mouse B cells.[44] We thus find that in human B cells, CIN85 negatively regulates BCR signaling via a Cbl-dependent mechanism. Our data obtained using CIN85-knockdown primary B cells also support this hypothesis. The molecular reason underlying the apparent discrepancy between our study and the aforementioned ones[42,43] remains unclear. One possibility, however, is that the relative contribution of CIN85-binding partners varies depending on the source of B cells used. In human B cells, Cbl proteins seem to preferentially associate with CIN85 over BLNK (Figure 1A). Notably, we found that CD2AP seems to preferentially associate with BLNK over c-Cbl in human B cells (supplemental Figure 2). It is therefore of potential interest

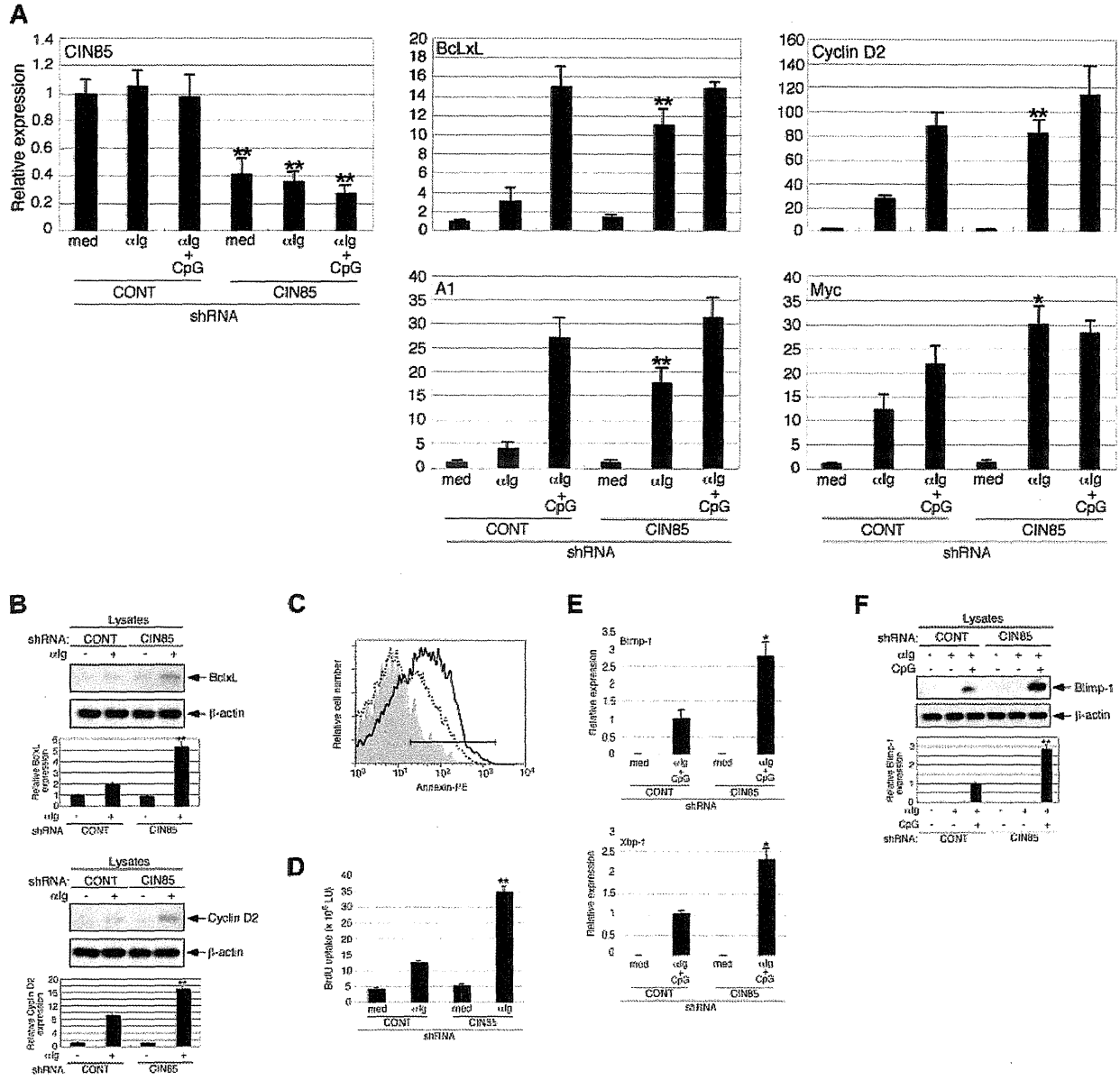

Figure 6. CIN85 knockdown enhances the survival, growth, and differentiation of primary B cells. (A) Control and CIN85-knockdown primary B cells were incubated for 24 hours in medium containing F(ab')$_2$ goat anti–human IgG/IgA/IgM (αIg, 20 μg/mL) or αIg plus CpG (1μM), and CIN85, BcLxL, A1, cyclin D2, and myc mRNA levels were quantified by real-time PCR. The data are normalized to the expression of 18S rRNA. The results shown are representative of 3 independent experiments (*$P < .05$, **$P < .01$ vs controls). (B) Control and CIN85-knockdown primary B cells were incubated for 24 hours in the absence or presence of F(ab')$_2$ goat anti–human IgG/IgA/IgM (αIg, 20 μg/mL). The cell lysates were subsequently separated on a SDS-PAGE gel and analyzed by Western blotting with anti-BclxL mAb, anti-cyclin D2 pAb, or anti–β-actin mAb. The resulting values are expressed as fold changes in protein expression compared with nonstimulated control cells. The values are the mean ± SD of 3 independent experiments (**$P < .01$ vs controls). (C) Control and CIN85-knockdown primary B cells were incubated for 48 hours in the absence or presence of F(ab')$_2$ goat anti–human IgG/IgA/IgM (αIg, 20 μg/mL). After culture, the cells were stained with PE-labeled annexin V and analyzed using flow cytometry. The percentages of annexin-positive cells are shown. A representative histogram of 3 independent experiments is shown. (D) Control and CIN85-knockdown primary B cells were incubated for 48 hours in the absence or presence of F(ab')$_2$ goat anti–human IgG/IgA/IgM (αIg, 20 μg/mL). After culture, the cells were pulsed with BrdU, and its incorporation was detected by incubation with anti-BrdU mAb, followed by rhodamine-conjugated anti–mouse Ab. A representative histogram of 3 independent experiments is shown (**$P < .01$ vs controls). (E) Control and CIN85-knockdown primary B cells were incubated for 48 hours in the absence or presence of F(ab')$_2$ goat anti–human IgG/IgA/IgM (αIg, 20 μg/mL) and CpG (1μM), and quantitation of Blimp-1 and Xbp-1 mRNA by real-time PCR was carried out. The data are normalized to the expression of 18S rRNA. The results shown are representative of 3 independent experiments (*$P < .05$ vs controls). (F) Control and CIN85-knockdown primary B cells were incubated for 48 hours with or without F(ab')$_2$ goat anti–human IgG/IgA/IgM (αIg, 20 μg/mL) in the absence or presence of CpG (1μM). The cell lysates were subsequently separated on a SDS-PAGE gel and analyzed by Western blotting with anti–Blimp-1 mAb or anti–β-actin mAb. The resulting values are expressed as fold changes in protein expression compared with unstimulated control cells. The values are the mean ± SD of 3 independent experiments (**$P < .01$ vs controls).

to compare the roles of CIN85 and CD2AP in the function of human B cells.

BCR signals play a pivotal role in the survival, growth, and differentiation of B cells.[1,2] Under physiologic conditions, BCR signaling is fine-tuned by positive and negative regulators and is generally insufficient for the full activation of B cells, rendering them susceptible to apoptosis and anergy. However, when the negative regulation of BCR signaling is compromised, unwanted B cells could grow and survive, thereby potentially leading to autoimmunity and B-cell malignancies. This study showed that

CIN85 knockdown in primary B cells causes full activation of B cells and enhances BCR-induced survival and growth via the increased expression of BcLxL, A1, cyclin D2, and myc (Figure 6). Given that Cbl proteins are critical for B-cell anergy,[10] CIN85 may cooperate with Cbl proteins to function as a key negative regulator for BCR signaling and to maintain self-tolerance. It is thus of interest to determine whether the expression and/or function of CIN85 could be altered in human autoimmune diseases such as SLE. Surprisingly, CLL cells from advanced-stage patients exhibit hypophosphorylation of c-Cbl,[11] as seen in CIN85-knockdown cells. The manipulation of CIN85 expression may therefore provide a novel strategy to control aberrant cell growth and survival in B-cell malignancies.

Acknowledgments

The authors thank Editage for proofreading the English used in this paper.

This work was supported in part by a Grant-in-Aid from the Ministry of Education, Culture, Sports, Science, and Technology of Japan (H.N. and K.A.).

Authorship

Contribution: H.N. and K.A. designed and performed the research, analyzed the data, and wrote the paper; S.J.-T., Y.K., T.S., K.N., S.-i.O., H. Tsuzuki, Y.I., Y.A., H.I., S.S., E.B., H. Tsukamoto, and T.H. performed the research; and T.T. provided cDNA constructs and helped write the paper.

Conflict-of-interest disclosure: The authors declare no competing financial interests.

Correspondence: Hiroaki Niiro, Dept of Medicine and Biosystemic Science, Graduate School of Medical Sciences, Kyushu University, 3-1-1 Maidashi, Higashi-ku, Fukuoka 812-8582, Japan; e-mail: hniiro@med.kyushu-u.ac.jp.

References

1. Niiro H, Clark EA. Regulation of B-cell fate by antigen-receptor signals. *Nat Rev Immunol.* 2002;2(12):945-956.
2. Kurosaki T, Shinohara H, Baba Y. B cell signaling and fate decision. *Annu Rev Immunol.* 2010;28: 21-55.
3. Pogue SL, Kurosaki T, Bolen J, Herbst R. B cell antigen receptor-induced activation of Akt promotes B cell survival and is dependent on Syk kinase. *J Immunol.* 2000;165(3):1300-1306.
4. Thien CB, Langdon WY. c-Cbl and Cbl-b ubiquitin ligases: substrate diversity and the negative regulation of signalling responses. *Biochem J.* 2005; 391(pt 2):153-166.
5. Liu YC, Gu H. Cbl and Cbl-b in T-cell regulation. *Trends Immunol.* 2002;23(3):140-143.
6. Swaminathan G, Tsygankov AY. The Cbl family proteins: ring leaders in regulation of cell signaling. *J Cell Physiol.* 2006;209(1):21-43.
7. Duan L, Reddi AL, Ghosh A, Dimri M, Band H. The Cbl family and other ubiquitin ligases: destructive forces in control of antigen receptor signaling. *Immunity.* 2004;21(1):7-17.
8. Panchamoorthy G, Fukazawa T, Miyake S, et al. p120cbl is a major substrate of tyrosine phosphorylation upon B cell antigen receptor stimulation and interacts in vivo with Fyn and Syk tyrosine kinases, Grb2 and Shc adaptors, and the p85 subunit of phosphatidylinositol 3-kinase. *J Biol Chem.* 1996;271(6):3187-3194.
9. Yasuda T, Maeda A, Kurosaki M, et al. Cbl suppresses B cell receptor-mediated phospholipase C (PLC)-gamma2 activation by regulating B cell linker protein-PLC-gamma2 binding. *J Exp Med.* 2000;191(4):641-650.
10. Kitaura Y, Jang IK, Wang Y, et al. Control of the B cell-intrinsic tolerance programs by ubiquitin ligases Cbl and Cbl-b. *Immunity.* 2007;26(5):567-578.
11. Mankai A, Eveillard JR, Buhe V, et al. Is the c-Cbl proto-oncogene involved in chronic lymphocytic leukemia? *Ann N Y Acad Sci.* 2007;1107:193-205.
12. Niiro H, Maeda A, Kurosaki T, Clark EA. The B lymphocyte adaptor molecule of 32 kD (Bam32) regulates B cell antigen receptor signaling and cell survival. *J Exp Med.* 2002;195(1): 143-149.
13. Niiro H, Allam A, Stoddart A, Brodsky FM, Marshall AJ, Clark EA. The B lymphocyte adaptor molecule of 32 kilodaltons (Bam32) regulates B cell antigen receptor internalization. *J Immunol.* 2004;173(9):5601-5609.
14. Take H, Watanabe S, Takeda K, Yu ZX, Iwata N, Kajigaya S. Cloning and characterization of a novel adaptor protein, CIN85, that interacts with c-Cbl. *Biochem Biophys Res Commun.* 2000; 268(2):321-328.
15. Gout I, Middleton G, Adu J, et al. Negative regulation of PI 3-kinase by Ruk, a novel adaptor protein. *EMBO J.* 2000;19(15):4015-4025.
16. Bogler O, Furnari FB, Kindler-Roehrborn A, et al. SETA: a novel SH3 domain-containing adapter molecule associated with malignancy in astrocytes. *Neuro Oncol.* 2000;2(1):6-15.
17. Narita T, Amano F, Yoshizaki K, et al. Assignment of SH3KBP1 to human chromosome band Xp22.1–>p21.3 by in situ hybridization. *Cytogenet Cell Genet.* 2001;93(1-2):133-134.
18. Petrelli A, Gilestro GF, Lanzardo S, Comoglio PM, Migone N, Giordano S. The endophilin-CIN85-Cbl complex mediates ligand-dependent downregulation of c-Met. *Nature.* 2002;416(6877):187-190.
19. Soubeyran P, Kowanetz K, Szymkiewicz I, Langdon WY, Dikic I. Cbl-CIN85-endophilin complex mediates ligand-induced downregulation of EGF receptors. *Nature.* 2002;416(6877):183-187.
20. Molfetta R, Belleudi F, Peruzzi G, et al. CIN85 regulates the ligand-dependent endocytosis of the IgE receptor: a new molecular mechanism to dampen mast cell function. *J Immunol.* 2005; 175(7):4208-4216.
21. Peruzzi G, Molfetta R, Gasparrini F, et al. The adaptor molecule CIN85 regulates Syk tyrosine kinase level by activating the ubiquitin-proteasome degradation pathway. *J Immunol.* 2007;179(4):2089-2096.
22. Marois L, Vaillancourt M, Pare G, et al. CIN85 modulates the down-regulation of Fc gammaRIIa expression and function by c-Cbl in a PKC-dependent manner in human neutrophils. *J Biol Chem.* 2011;286(17):15073-15084.
23. Tabrizi SJ, Niiro H, Masui M, et al. T cell leukemia/lymphoma 1 and galectin-1 regulate survival/cell death pathways in human naive and IgM+ memory B cells through altering balances in Bcl-2 family proteins. *J Immunol.* 2009;182(3):1490-1499.
24. Narita T, Nishimura T, Yoshizaki K, Taniyama T. CIN85 associates with TNF receptor 1 via Src and modulates TNF-alpha-induced apoptosis. *Exp Cell Res.* 2005;304(1):256-264.
25. Havrylov S, Rzhepetskyy Y, Malinowska A, Drobot L, Redowicz MJ. Proteins recruited by SH3 domains of Ruk/CIN85 adaptor identified by LC-MS/MS. *Proteome Sci.* 2009;7:21.
26. Watanabe S, Take H, Takeda K, Yu ZX, Iwata N, Kajigaya S. Characterization of the CIN85 adaptor protein and identification of components involved in CIN85 complexes. *Biochem Biophys Res Commun.* 2000;278(1):167-174.
27. Chiu CW, Dalton M, Ishiai M, Kurosaki T, Chan AC. BLNK: molecular scaffolding through 'cis'-mediated organization of signaling proteins. *EMBO J.* 2002;21(23):6461-6472.
28. Marshall AJ, Niiro H, Yun TJ, Clark EA. Regulation of B-cell activation and differentiation by the phosphatidylinositol 3-kinase and phospholipase Cgamma pathway. *Immunol Rev.* 2000;176:30-46.
29. Turner M. B-cell development and antigen receptor signalling. *Biochem Soc Trans.* 2002;30(4): 812-815.
30. Peng SL, Gerth AJ, Ranger AM, Glimcher LH. NFATc1 and NFATc2 together control both T and B cell activation and differentiation. *Immunity.* 2001;14(1):13-20.
31. Rao N, Ghosh AK, Ota S, et al. The non-receptor tyrosine kinase Syk is a target of Cbl-mediated ubiquitylation upon B-cell receptor stimulation. *EMBO J.* 2001;20(24):7085-7095.
32. Sohn HW, Gu H, Pierce SK. Cbl-b negatively regulates B cell antigen receptor signaling in mature B cells through ubiquitination of the tyrosine kinase Syk. *J Exp Med.* 2003;197(11):1511-1524.
33. Su TT, Rawlings DJ. Transitional B lymphocyte subsets operate as distinct checkpoints in murine splenic B cell development. *J Immunol.* 2002; 168(5):2101-2110.
34. Yi AK, Chang M, Peckham DW, Krieg AM, Ashman RF. CpG oligodeoxyribonucleotides rescue mature spleen B cells from spontaneous apoptosis and promote cell cycle entry. *J Immunol.* 1998;160(12):5898-5906.
35. Calame KL, Lin KI, Tunyaplin C. Regulatory mechanisms that determine the development and function of plasma cells. *Annu Rev Immunol.* 2003;21:205-230.
36. Turner M, Schweighoffer E, Colucci F, Di Santo JP, Tybulewicz VL. Tyrosine kinase SYK: essential functions for immunoreceptor signalling. *Immunol Today.* 2000;21(3):148-154.

37. Stamenova SD, French ME, He Y, Francis SA, Kramer ZB, Hicke L. Ubiquitin binds to and regulates a subset of SH3 domains. *Mol Cell.* 2007; 25(2):273-284.

38. Shimokawa N, Haglund K, Holter SM, et al. CIN85 regulates dopamine receptor endocytosis and governs behaviour in mice. *EMBO J.* 2010; 29(14):2421-2432.

39. Stoddart A, Dykstra ML, Brown BK, Song W, Pierce SK, Brodsky FM. Lipid rafts unite signaling cascades with clathrin to regulate BCR internalization. *Immunity.* 2002;17(4):451-462.

40. Jacob M, Todd L, Sampson MF, Pure E. Dual role of Cbl links critical events in BCR endocytosis. *Int Immunol.* 2008;20(4):485-497.

41. Zhang M, Veselits M, O'Neill S, et al. Ubiquitinylation of Ig beta dictates the endocytic fate of the B cell antigen receptor. *J Immunol.* 2007;179(7): 4435-4443.

42. Oellerich T, Bremes V, Neumann K, et al. The B-cell antigen receptor signals through a preformed transducer module of SLP65 and CIN85. *EMBO J.* 2011;30(17):3620-3634.

43. Kometani K, Yamada T, Sasaki Y, et al. CIN85 drives B cell responses by linking BCR signals to the canonical NF-kappaB pathway. *J Exp Med.* 2011;208(7):1447-1457.

44. Buchse T, Horras N, Lenfert E, et al. CIN85 interacting proteins in B cells-specific role for SHIP-1. *Mol Cell Proteomics.* 2011;10(10):M110.

Regular Article

LYMPHOID NEOPLASIA

PU.1 is a potent tumor suppressor in classical Hodgkin lymphoma cells

Hiromichi Yuki,[1] Shikiko Ueno,[1] Hiro Tatetsu,[1] Hiroaki Niiro,[2] Tadafumi Iino,[2] Shinya Endo,[1] Yawara Kawano,[1] Yoshihiro Komohara,[3] Motohiro Takeya,[3] Hiroyuki Hata,[1] Seiji Okada,[4] Toshiki Watanabe,[5] Koichi Akashi,[2] Hiroaki Mitsuya,[1] and Yutaka Okuno[1]

[1]Department of Hematology, Kumamoto University of Medicine, Kumamoto, Japan; [2]Medicine and Biosystemic Science, Kyushu University Graduate School of Medical Sciences, Fukuoka, Japan; [3]Department of Cell Pathology, Kumamoto University of Medicine, Kumamoto, Japan; [4]Division of Hematopoiesis, Center for AIDS Research, Kumamoto University, Kumamoto, Japan; and [5]Graduate School of Frontier Sciences, University of Tokyo, Tokyo, Japan

Key Points

- PU.1 is a potent tumor suppressor in cHL cells and the induction of PU.1 is a possible therapeutic option for patients with cHL.

PU.1 has previously been shown to be down-regulated in classical Hodgkin lymphoma (cHL) cells via promoter methylation. We performed bisulfite sequencing and proved that the promoter region and the −17 kb upstream regulatory element of the *PU.1* gene were highly methylated. To evaluate whether down-regulation of PU.1 is essential for the growth of cHL cells, we conditionally expressed PU.1 in 2 cHL cell lines, L428 and KM-H2. Overexpression of PU.1 induced complete growth arrest and apoptosis in both cell lines. Furthermore, in a Hodgkin lymphoma tumor xenograft model using L428 and KM-H2 cell lines, overexpression of PU.1 led to tumor regression or stable disease. Lentiviral transduction of PU.1 into primary cHL cells also induced apoptosis. DNA microarray analysis revealed that among genes related to cell cycle and apoptosis, *p21 (CDKN1A)* was highly up-regulated in L428 cells after PU.1 induction. Stable knockdown of p21 rescued PU.1-induced growth arrest in L428 cells, suggesting that the growth arrest and apoptosis observed are at least partially dependent on p21 up-regulation. These data strongly suggest that PU.1 is a potent tumor suppressor in cHL and that induction of PU.1 with demethylation agents and/or histone deacetylase inhibitors is worth exploring as a possible therapeutic option for patients with cHL. (*Blood.* 2013;121(6):962-970)

Introduction

Hodgkin lymphoma is a B-cell malignancy that occurs frequently in the white population, and is relatively rare within Japanese and other Asian populations.[1] To date, the combination of chemotherapy and irradiation has led to a dramatic improvement in both progression-free survival and overall survival of stage I and II patients, which now exceeds 90%.[2] In contrast, the prognosis of the remaining patients who relapse or fail to make complete remission, and in stage III and IV patients, is relatively poor.[3-9] In addition, patients who achieve long-term disease-free survival frequently have infertility and secondary malignancies, including breast cancer and cardiac failure, which are related to chemotherapeutic agents and radiation therapies.[10-12] Therefore, the development of new therapeutic strategies is necessary to improve clinical outcome and reduce the long-term side effects of current treatments in these patients. Nevertheless, our understanding of the mechanisms underlying the pathogenesis of Hodgkin lymphoma, which are necessary for the generation of novel, molecularly targeted agents, remains incomplete. It is known that both alleles of *tumor necrosis factor, α-induced protein 3 (TNFAIP3)*(*A20*) are deleted in a third of patients with Hodgkin lymphoma of nodular sclerosis histology and in the classic Hodgkin lymphoma (cHL) cell line, KM-H2.[13]

Hodgkin lymphoma is subdivided into cHL, which constitutes the majority of patients (95%), and nodular lymphocyte predominant Hodgkin lymphoma.[1] In cHL, lymphoma cells do not express the B cell–specific surface antigens, CD19 and CD20, or the B cell–specific transcription factors, Bob.1, PU.1, and SpiB.[14,15]

PU.1 is an Ets family transcription factor that is essential for the differentiation of both myeloid and lymphoid cells.[16,17] PU.1 is expressed in granulocytes, monocytes/macrophages, and B cells, but not in erythrocytes or T cells. The expression of *PU.1* requires an upstream regulatory element (URE) located −14 kb and −17 kb upstream of the transcriptional start site of the murine and human *PU.1* genes, respectively, in addition to promoter regulatory elements.[18-20] In murine models, deletion of the −14 kb URE led to down-regulation of PU.1 expression to 20% of wild-type mice, and surprisingly, knockout mice developed acute myeloid leukemia and a B-cell chronic lymphocytic leukemia-like disease.[21,22] These data suggest that PU.1 has tumor suppressor activity in myeloid cells and B cells. We recently reported that PU.1 is down-regulated in a subset of multiple myeloma cells and in most myeloma cell lines. Conditional expression of PU.1 induced complete growth arrest and apoptosis in myeloma cell lines, suggesting that PU.1 is a potent tumor suppressor in multiple myeloma.[20]

Submitted May 21, 2012; accepted October 30, 2012. Prepublished online as *Blood* First Edition paper, December 4, 2012; DOI 10.1182/blood-2012-05-431429.

The online version of this article contains a data supplement.

The publication costs of this article were defrayed in part by page charge payment. Therefore, and solely to indicate this fact, this article is hereby marked "advertisement" in accordance with 18 USC section 1734.